Universität Bremen
Faculty of Environmental Physics

Master Thesis

True Coincidence Summing Correction in Gamma Spectroscopy

Wissam Chehade

7th September 2007

Supervisor:Dr. Helmut Fischer

Referee: Prof. Dr. Jörn Bleck-Neuhaus

Contents:

CHAPTER 3

Implementation of Cascade Corrections in Genie 2000

CHAPTER 4

Results, Validations and Discussions

Acknowledgements

My recognition to the leading and all the teaching faculty of the IUP, for the inspiration and motivation I gained in perusing the course.

My gratitude to Dr. Helmut Fischer for supervision and guidance, and my group members for assistance that kept me progressive throughout my thesis work.

My special thanks to special friends for all the dynamic support and last but not least my family for all the upholding encouragement.

Abstract

In environmental or low-level γ-ray spectrometry, the determination of activities or application of efficiency curves is hampered by the phenomenon of true coincidence summing. It is intended to bring the sample close to the detector and the probability of the detector to register two photons emitted by the same decaying nucleus as one is no longer negligible. All this becomes even more complex when the sample's specific activity is so low that it is essential to measure a larger volume of sample material. In that case, the detector efficiency can no longer be considered constant over the source volume and the voluminous true-coincidence summing effect comes into play. Completely neglecting true coincidence summing effects when identifying isotopes may result in negative consequences, such as biased result for radionuclide activities and the associated uncertainties, and missed or falsely identified radionuclides.

A simple procedure for correction for cascade summing can be achieved by obtaining the peak-to-total ratio for the HPGe detector.These ratios are measured using single line emitters placed at an arbitrary distance from the detector.

This procedure saves money and time since only a set of uncallibrated point sources are needed to obtain the P/T ratios for a detector.
Results obtained are improved to within 5% of the true value.

List of Figures:

List of Tables:

1

Semiconductor Detectors for Gamma-Ray Spectroscopy

1.1 Introduction

Gamma spectroscopy is a radioanalytical measurement technique, the best for identification and quantification of radionuclides using germanium detectors, while a Geiger counter determines only the count rate, a gamma spectrometer will determine the energy and the count rate of gamma rays emitted by radioactive substances. This is due to the characteristic discrete energies of gamma-rays produced by radioisotopes, which is the basics of gamma spectroscopy (Gammas and X-rays are usually properties of the daughter nucleus). By measuring the energies of gamma ray photons, the source of radiation can be determined by comparison of the observed photopeaks to a library of known gamma emitting source energies. The net count in

the photopeak area is related to element activity or concentration of the radioisotope. The method is thus a powerful tool for monitoring the radiation environment.
The combination of absorption coefficient, semiconductor properties and availability in a suitably pure state makes germanium the predominant material for high-resolution gamma-ray detectors.

1.2 General Consideration in Gamma-Ray Spectroscopy

An X-ray or gamma-ray photon is uncharged and creates no direct ionization or excitation of the material through which it passes contrary to charged particles (e.g. alpha and beta). The detection of gamma rays is therefore critically dependent on causing the gamma-ray photon to undergo an interaction that transfers all or part of the photon energy to charged particles in the absorbing material which can be collected together to produce an electrical signal.

The detection of gamma rays depends on interactions as photoelectric effect, Compton scattering and pair production, which transfer gamma ray energy to electrons within the detector material. The excited electrons then lose energy by ionization. These charged pairs produced by the primary electrons are electron-hole pairs whose number corresponds to the energy of primary electrons. The detector must be constructed of suitable material so that the electron hole pairs can be collected and presented as electrical signal.

The properties that should be considered for an ideal detector for gamma spectroscopy are;

- Output proportional to gamma-ray energy.
- Good efficiency, i.e. high absorption coefficient
- Easy mechanism for collecting the detector signal
- Good stability over time, temperature and operating parameters
- Reasonable cost
- Reasonable size

1.3 Gamma-Ray Spectroscopy with Semiconductor Detector

For a detector serving as a gamma-ray spectrometer, it must carry out two distinct functions; i.e. first it must act as a conversion medium with reasonable probability of gamma ray interaction yielding one or more fast primary electrons; second, it must function as a conventional detector for secondary electrons.

The requirement of full absorption of the secondary electron rules out gas-filled detectors for the spectroscopy of gamma rays, other than those with very low energy. The penetration distance of a 1 MeV electron in standard temperature and pressure (STP) gases is several meters, so that detectors of any practical size can never come close to absorbing all the secondary electron energy.

For the measurement of gamma rays above several hundred keV, there are two detector categories of major importance, inorganic scintillators as NaI(Tl) and semiconductor detectors.

The scintillators have the advantage of availability in large size and high density which can result in high interaction probabilities for gamma-rays. Due to the high atomic number of iodine, a large number of all interactions will result in complete absorption of gamma-ray energy, so the photo fraction will be high.
The energy resolution of scintillators is poor.

Figure-1.1 shows comparative spectra with germanium and shows that it is better choice for separation of closely spaced gamma energies. The typical energy resolution of a good germanium system is few tenths of a percent compared to 5-10 % for sodium iodide.

The smaller size available and the lower atomic number of germanium contribute to give photopeak efficiencies an order of magnitude lower in typical cases. Moreover the photofractions are low and thus the quanta in the pulse height spectra are more of a problem. On the other hand, the good resolution of the semiconductor detectors aids in the detection of weak sources of discrete energies when superimposed on a broad continuum.

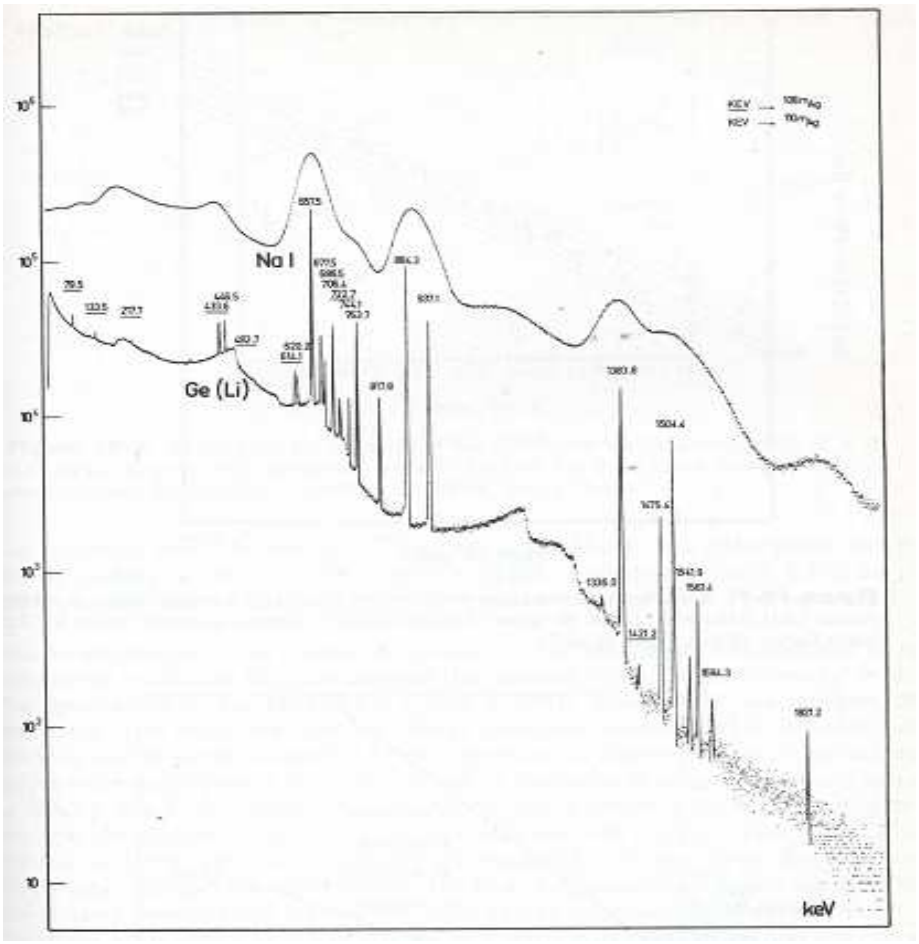

Figure 1.1 Comparative pulse height spectra recorded using NaI and Ge(Li) [1]

1.4 High Purity Germanium Detector

1.4.1 Introduction

The semiconductor materials are good for the electron-hole pair collection within the detector, this must be done within a reasonably short time. Moreover there must be no traps which can prevent them reaching the collecting contacts. Trapping centres can be due to

- Impurities within the semiconductor lattice
- Interstitial atoms and vacancies within the lattice due to structural defects
- Interstitial atoms caused by radiation damage

This implies that the detector material should be of high purity and nearly perfect crystalline state.

Germanium is the most commonly used detector material for its higher atomic number (as compared to Silicon) which makes it practicable for detection of higher energy gamma radiation. Over recent years, the technology for the manufacture of high purity germanium with a suitable degree of crystal perfection is achieved. When an n+ layer is created on a face of a high-purity p-type germanium slab (Figure-1.2) and a reverse bias is applied to the detector, a depletion layer throughout the p-type material is formed. Such a detector is called hyper-pure or simply high-purity germanium detector abbreviated as HPGe.

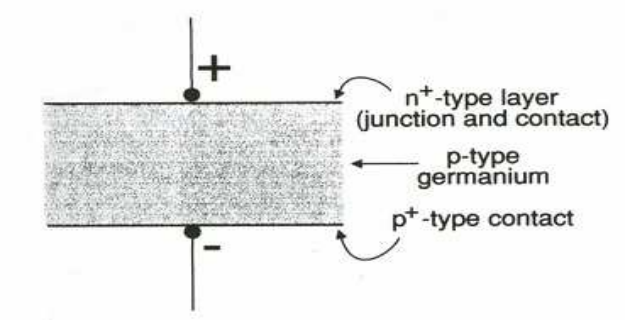

Figure 1.2 The basic construction of germanium detector. [1]

HPGe detectors are available in a number of different configurations to suit particular situations. Figure-1.3 shows the simple standard forms together with an indication the energy range over which they might be used.

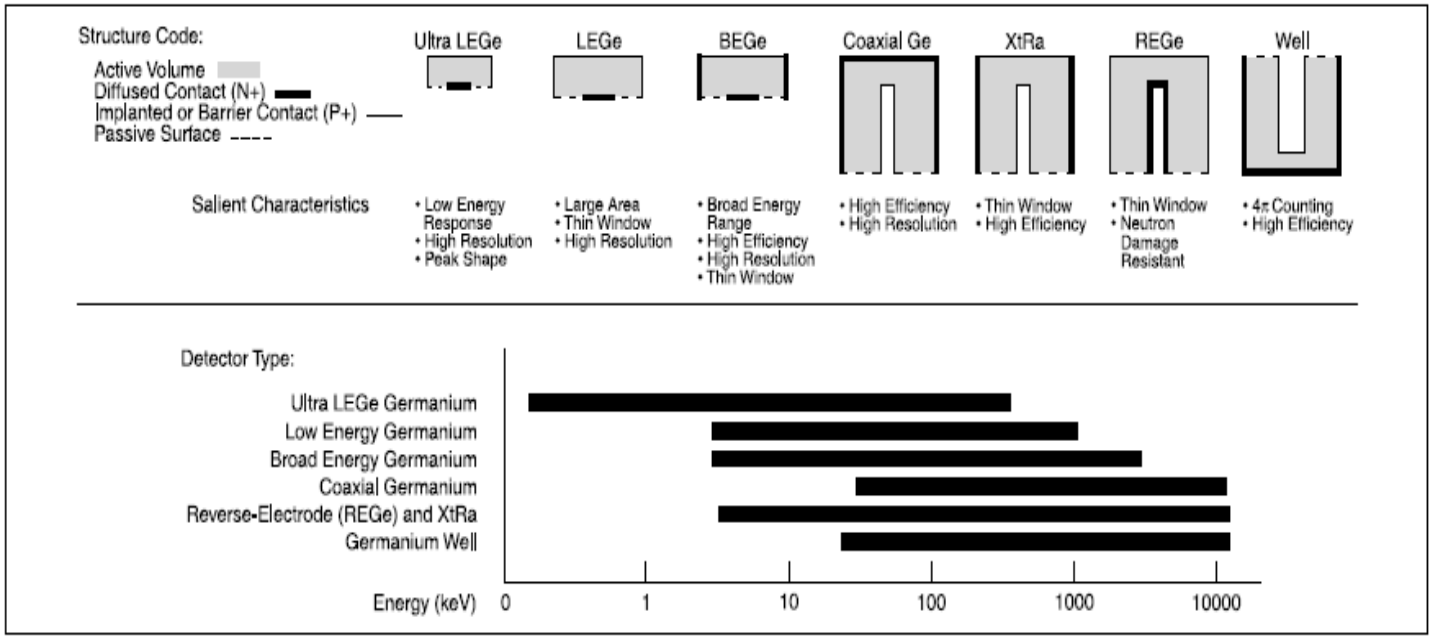

Figure 1.3 Configuration of detector generally available together with the used energy range [3]

1.4.2 Packing of the Detector

HPGe detectors are maintained within an evacuated metal container (usually aluminum) referred to as the can. The detector crystal inside the can is in thermal contact with a metal rod called a cold finger. The combination of metal container and cold finger is called the cryostat. The cold finger extends past the vacuum boundary of the cryostat into a Dewar flask that is filled with liquid nitrogen. The immersion of the cold finger into the liquid nitrogen maintains the HPGe crystal at a constant low temperature. This helps to ensure the reproducibility of the electronic measurement (reduce electronic noise) and thereby achieve as a high resolution as possible. The construction of the cryostat must take into account a number of factors;

- The detector should be maintained at a temperature close to 77 K
- The detector cap must be thin enough to allow the gamma-radiation to penetrate but still withstand the vacuum and provide a reasonable degree of protection to the detector
- The cryostat construction must isolate the detector from mechanical vibration
- The cryostat's material should be specially selected if the detection system is set for low background measurements
- The detector must be kept under a clean vacuum to prevent condensation on the detector. There must be electrical feed-troughs to take the signal from the detector.

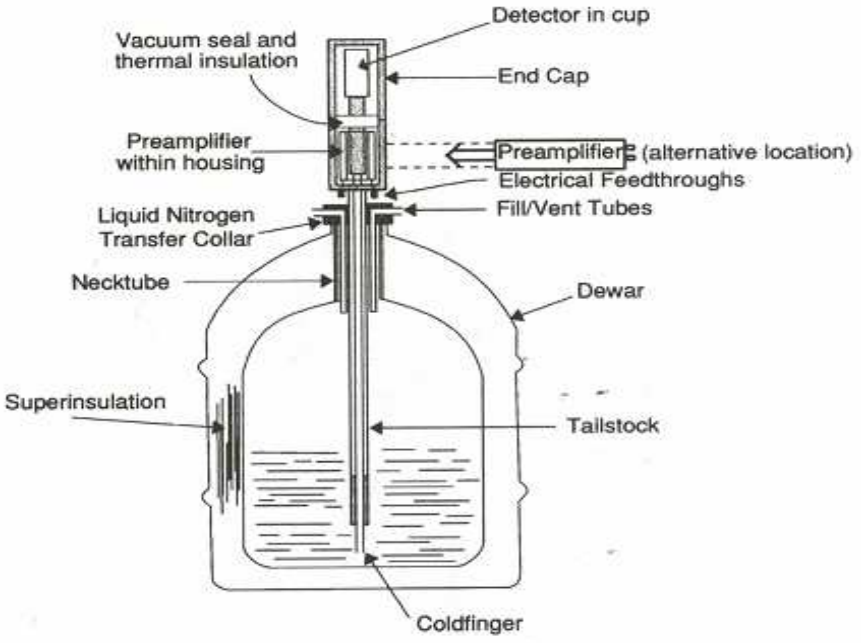

Figure 1.4 A typical germanium detector, cryostat and liquid nitrogen reservoir [3]

1.4.3 Detector Requirements and Characteristics

The spectra displayed for HPGe detector is characterised by a high energy resolution. The detector's resolution for a peak is defined as the FWHM at the peak's centroid (H_0) (Figure-1.5 (a)). The full width at half maximum (FWHM) of the gamma peak is expressed in keV. Higher resolution (smaller FWHM) means that the system has the ability to separate the peaks within the spectrum.

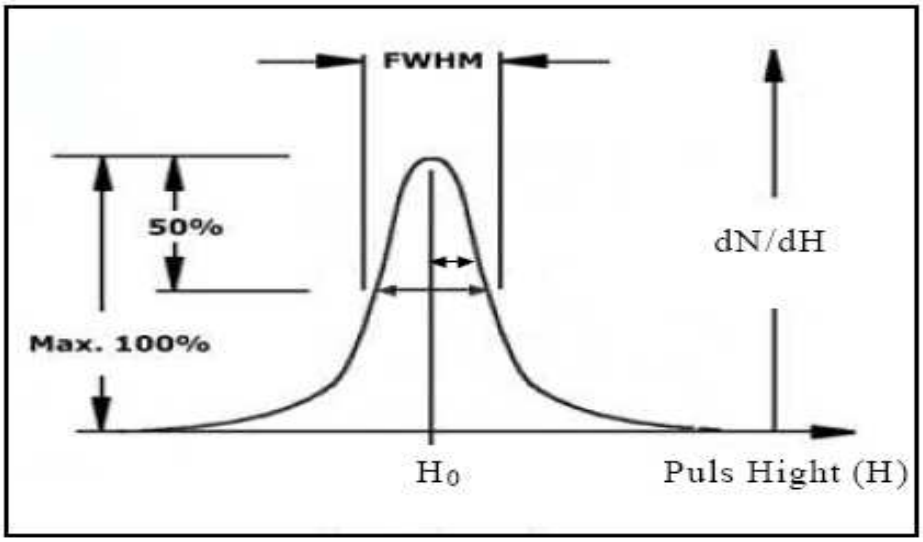

Figure 1.5 (a) A Display of The FWHM of a peak [4]

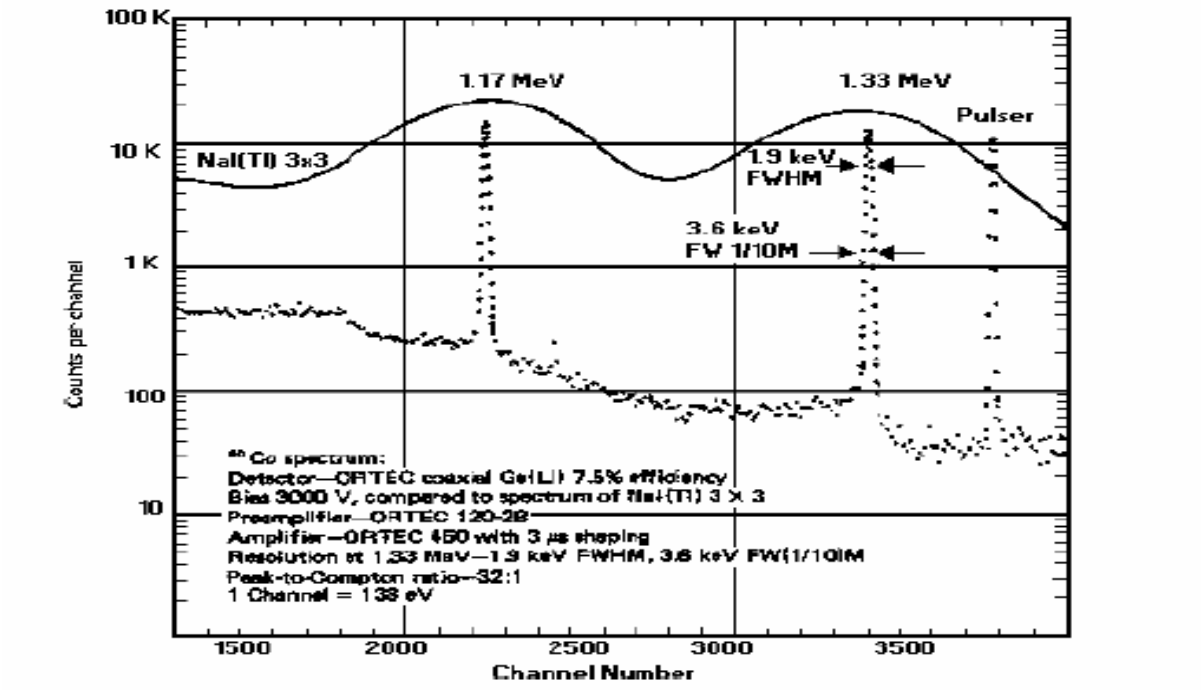

Figure 1.5 (b) Energy spectrum of Co-60 [4]

The FWHM is a function of energy and the Table 1.1 identifies how it will change for a particular detector as a function of energy.

Table 1.1 Typical FWHM values as a function of energy of a medium efficiency (30-50%) detector [8]

Energy, keV	100	600	1300
FWHM, keV	1.3	1.8	2.1

Peak-height-to-Compton ratio is another spectral parameter which is much improved for HPGe over NaI(Tl). The value for HPGe is between 30 and 50, compared to typically 9 for the NaI(Tl) detector

Operating Voltage

- The germanium detector has a voltage applied directly to the crystal (1000-5000V DC)
- The voltage supply unit for the detector should be on a line Conditioner so that small variations in line voltage are normalized to a constant voltage.
- Powering up a detector needs to be performed in a controlled manner at 50-100 volts/second to minimize shock to the detector crystal and maintain its performance

Shielding

- Detectors need to be shielded from external radiation, such as naturally occurring radionuclides emitted from building materials (particularly concrete).
- Shielding should be constructed of old lead because the old steel fabricated after the World war II contains traces of Co-60.
- The inner surfaces of these shields typically are lined with Cadmium then Copper to reduce lead X-rays and backscatter photons originating from the shield walls.

Background

Detectors have a certain background count rate from naturally occurring radionuclides, cosmic radiation, and the radioactivity in the detection equipment. The specific background gamma radiation will depend on the amounts of the nuclides present and on the sensitivity of the detector to the specific gamma rays. Ideally, the material used for shielding should itself be free of any radioactive material that might contribute to the background.

Temperature and Humidty

Humidity can have significant effects on the many cable connections that germanium detection systems have.

- The change in moisture can affect cable connection impedance, which ultimately can affect peak shape.
- The counting room should be maintained at 40-60 percent relative humidity.

There are two separate temperature effects that can be seen.

- The first deals with the detector itself. The band gap in the germanium crystal is affected by the absolute temperature, so it is maintained at -196 ˚C using a cryostat. The cryostats are designed to have minimum thermal leakage.
- The other temperature effect is that of the room environment on the electronics. Although the detector and the electronics may be on a conditioned line, the instability of temperature in the room can cause the pre-amplifier, amplifier, and ADC/PHA portions of the system to respond erratically. The temperature of the room should be maintained in the 21-27 ˚C range

1.5 Electronics for Gamma-Ray Spectrometry

The General Electronic System

The output from a gamma-ray detector is an amount of electrical charge proportional to the amount of gamma-ray energy absorbed by the detector. The function of the electronic system is to collect that charge, measure the amount and store the information. A typical simple electronic system for gamma-ray spectroscopy is shown in Figure-1.6.

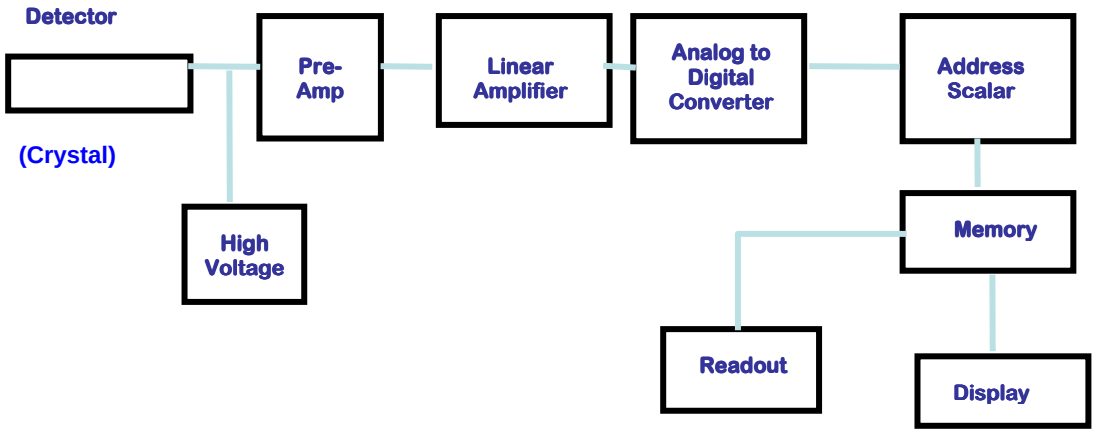

Figure 1.6 A simple schematic electronic system for gamma spectroscopy

The gamma photons produce electron-hole pairs and the electrons and holes are collected by an applied electrical field supplied by the bias supply. The charge-sensitive pre-amplifier detects the charge produced in the crystal, and produces an electrical pulse suitable for direct amplification. The linear amplifier changes the pulse shape and increases it size. The multichannel analyzer (MCA) sorts the pulses by the pulse height and counts the number of pulses within individual pulse height intervals called channel. Each of these units will be explained briefly.

Preamplifier

It collects the charge created within the detector by interaction with gamma-radiation and interfaces the detector to the amplifier. It provides a high impedance load for the detector and a low impedance source for the amplifier. The general modes of operation of preamplifiers used in high resolution gamma spectroscopy using semiconductor detector is the charge sensitive (others are current sensitive and voltage sensitive modes). Charge sensitive mode is advantageous in terms of noise performance and the gain is independent of the detector capacitance.

Amplifier

The sharp peaked pulses coming from preamplifiers are not suitable for direct measurement of peak height. For measurement purpose, the ideal pulse would be one gradually approaching a relatively flat top and falling away to the baseline as rapidly as possible. The pile-up of pulses with identical step height produces peak voltages at different heights. The pulse height is proportional to the gamma ray energy absorbed and extraction of information is favourable for rising edges of narrow peaked pulses. This task is accomplished by electronic filtering, also referred to as shaping.

Though amplifiers perform shaping, but there can be undesirable consequences associated with this task e.g. impairing resolution

MCA

The Multichannel Analyzer is a device that separates pulses based on pulse height. Each energy range of pulse height is referred to as a channel. The pulse height is proportional to the energy lost by a gamma photon. Separation of the pulses, based on pulse height, shows the energy spectrum of the gamma rays

that are emitted. Multichannel analyzers typically have 4k or 8k channels over an energy range of 0 to 2 MeV (the energy range depends on the amplifier gain setting). The output is a plot of pulse counts versus gamma energy. By analyzing the spectrum of gamma rays emitted, the user can determine the nuclidess which caused the gamma pulses.

The present day MCA works as a multifunctional device, dealing with many aspects of data analysis, such as collection and sorting pulses, storing and sorting data, data display, data analysis and preparation of data for output. The output is in the form of a display of the number of counts shown on y-axis and the corresponding channel number displayed on x-axis.

1.6 Counting statistics

The contents (N) of the observed γ lines are numbers resulting from a counting experiment, which are partially superimposed on a high background. This produces an uncertainty of the result which can seriously degrade the precision with which the net peak counts is measured. Counting statistics is applied to estimate this uncertainty which is expressed by the standard deviation of the result.
For any counting experiment the result (**N**) of which is governed by a Poisson distribution, the standard deviation is

$$\sigma = \sqrt{N} \qquad \textbf{(1.1)}$$

The above equation expresses the fact that a repetition of a counting experiment would in about 2/3 of the cases give a result in the range of N ± σ.

For the analysis of a peak without background this is sufficient. But to subtract a background, the Poisson distribution should be approximated by a Gaussian distribution. This can be done without large errors for numbers of counts (N) greater than about 10. In this case,

$$N_{net} = N_{tot} - N_{BG} \qquad \textbf{(1.2)}$$

$$\sigma = \sqrt{\sigma_{Ntot}^{\,2} + \sigma_{BG}^{\,2}} = \sqrt{N_{tot} + N_{BG}} \qquad \textbf{(1.3)}$$

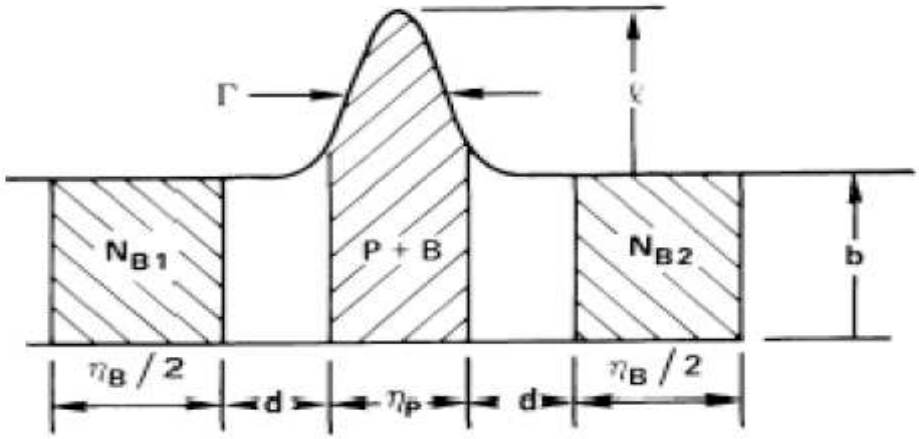

Figure 1.7 Peak and background areas for background subtraction [5]

In many cases the background has a slope. Therefore the counts in the background areas have to be determined at both sides of the peak and averaged. By such calculation, the value and the statistical error of the activity concentration can be determined.

1.7 Calibrations

The modern digital gamma ray spectrum displays number of pulses measured within small consecutive pulse height ranges. The detector is calibrated to interpret the spectrum in terms of energy rather than channel number or voltage and amount of radionuclides rather than number of pulses. A complicated spectrum analysis may need providing information about peak width variation and shape with energy or channel number. Therefore two main tasks have to be performed

.

- Energy calibration - the relationship between channel and energy
- Efficiency calibration - the relationship between number of counts and disintegration rate.

1.7.1 Energy Calibration

The energy calibration specifies the relationship between peak position in the spectrum (channel number) and the corresponding gamma-ray energy. This is accomplished by measuring the spectrum of a source emitting gamma-rays of

precisely known energy and comparing the measured peak position with energy irrespective of the number of nuclides present in the source. For any source, it should be ensured that the calibration energies cover the entire range over which the spectrum is to be used.
In practice, the spectrum should be measured long enough to achieve good statistical precision for the peaks to be used for calibration.

Figure-1.8 shows an energy calibration using Eu-152. 55 points are plotted together with the best fit straight line though normally the spectrometer from which the data of Figure-1.8 were obtained would be calibrated only few points marked. The data appear to fit the linear relationship very well.

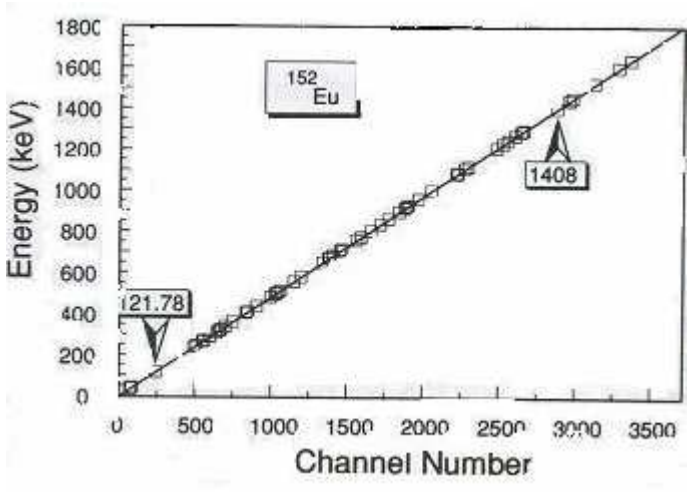

Figure 1.8 Energy Calibration.

$$E\ (keV) = I+GC \qquad \textbf{(1.4)}$$

Where I and C are intercept and gradient of calibration line and C is the channel position. The applicability of equation 1.4 depends on the integral linearity of gamma spectrometer system and the use to which the information is to be put. Over most of the spectrum, the errors are small and are most likely to occur at the extremes of the energy scale.

1.7.2 Efficiency Calibration

What is meant by efficiency depends on how it is used; three efficiencies can be considered;

- **Absolute full-peak energy efficiency**: This efficiency relates the peak area in the spectrum to the number of gamma rays emitted by the source. It depends on geometrical arrangement of source and detector.
- **Absolute total efficiency**: This efficiency relates the number of gamma-rays emitted by the source to the number of counts detected anywhere in the spectrum taking into account the full energy peak and all incomplete absorptions represented by Compton continuum.
- **Intrinsic efficiency**: This efficiency relates the counts in the peaks of the spectrum to the number of gamma-rays incident on the detector. This efficiency is independent of source/detector geometry.

Full Energy Peak Efficiency

This parameter is of most significance in practical gamma-spectroscopy and is given by:

$$\varepsilon = R/(S.f_{\gamma}) \qquad \textbf{(1.5)}$$

where R is the full energy peak count rate in counts per seconds, S the source strength in disintegrations per seconds (Bq) and f_{γ} is the probability of emission of the particular gamma-ray being measured.

It is convenient to construct an efficiency curve by measuring many gamma rays and plotting the efficiency versue energy to provide the efficiency data needed by the inverse of equation 1.5 to convert peak area to activity. Generally point sources emit single gamma rays at low count rates and reasonably large source detector distance. There are several reasons for the irrelevance of such a calibration curve in practice;

- Different source to detector distance
- Different shape of source
- Absorption within the source
- Random summing at high count rate
- True coincident summing at close geometry
- Decay of source during counting
- Electronic timing problems

For environmental measurement that involve a limited set of radionuclides, it would be better to make the measurements relative to a reference standard for each nuclide rather than depending on upon interpolation of a calibration curve. This interpolation introduces extra uncertainties added to those involved in producing a point on the curve. Due to the above mentioned factors, the calibration curve may not be accurate. If the spectrum analysis program requires a calibration curve, then a curve must be created. However, the following correction factors should be considered in using calibration curves;

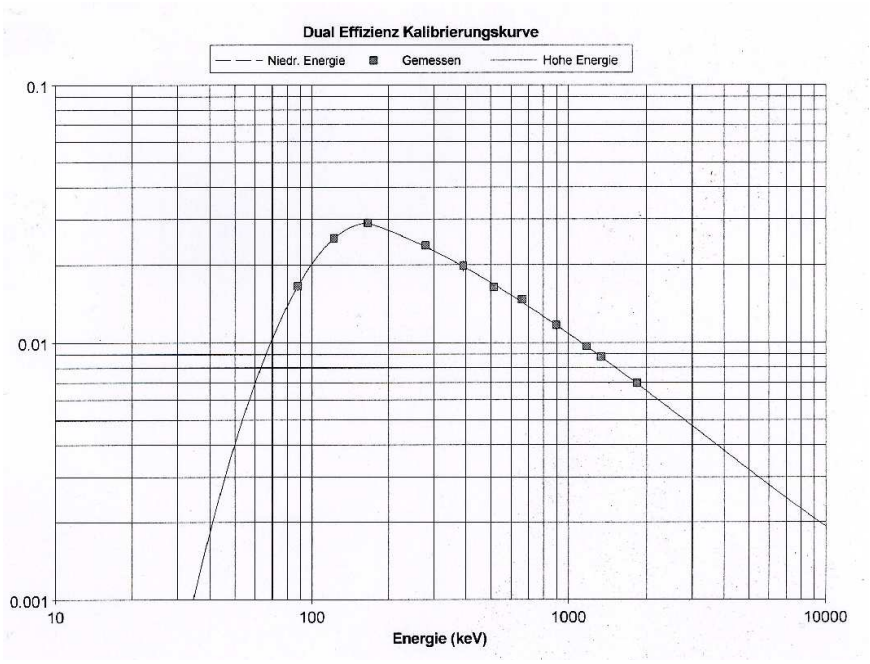

Figure-1.9 Full peak energy calibration curve for a Marinelli Beaker

i. Dead-time correction

The dead-time correction factor is $(1\text{-}R\tau)^{-1}$, where τ is the dead-time value selected for the dead-time module and R is the total count rate above the threshold including the digital overflows. Such factor depends on the sample's count rate.

ii. Pile-up correction

A pulse will be counted and stored whenever it is not followed or preceded by another pulse during a certain period of time τ, the resolution time of the electronic system. Using the Poisson distribution, the probability of a random coincidence, p_c, within τ is;

$$p_c = 1 - e^{-2R\tau} \quad \textbf{(1.6)}$$

R is the mean count rate

If A is the measured peak area and A_T is the true peak area,

$$(A_T - A)/A_T = p_c = 1 - e^{-2R\tau} \quad \textbf{(1.7)}$$

Rearranging equation (1.7), we can derive a simple equation to correct peak areas for random summing

$$A_T = A\, e^{-2R\tau} \quad \textbf{(1.8)}$$

iii. True coincidence summing

The source of such error is due to the summing of gamma-rays emitted simultaneously from the nucleus. This error is prominent when measurements involving nuclides with complicated decay scheme are conducted. True coincidence summing is geometry dependent and errors are particularly severe when sources are positioned very close to the detector. For this reason, the close geometry efficiency curve requires single-gamma-ray sources. The origin of true coincident summing, the need for its correction and the aspects dealing with how to find the corrections is the main topic of the present work are discussed in Chapter 2.

2

True Coincidence Summing

2.1 Introduction

Gamma spectroscopy using HPGe detectors is commonly used for its high energy resolution. It can be used for the activity determination of gamma-emitting radioactive sources provided the full-peak efficiency calibration curve is known. In that case, the efficiency value for each gamma ray energy is obtained by interpolation. The measured peak efficiency curves should be corrected for cascade summing due to simultaneous detection of two or more gamma-rays from the same decay event inside the detector crystal.

When the gamma rays arrive within the width of the amplifier output pulse they will not be recognized as separate events. The resulting output pulse will be equivalent to the height of the first pulse received plus the height of the second pulse. This situation is demonstrated in Figure-2.1, in which the calculated preamplifier and

amplifier output pulses shapes are plotted when the pulses arrive at the preamplifier input. The diagram shows that for every coincidence, the height of the combined output pulse measured at MCA, is the sum of the two pulses heights.

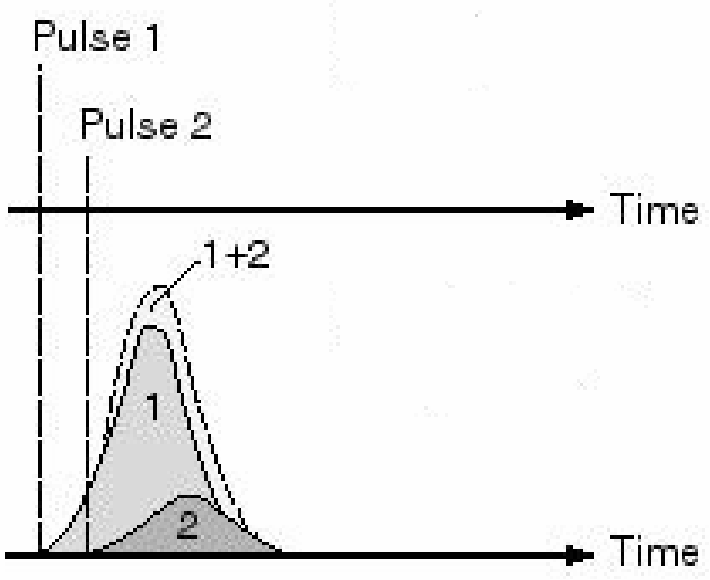

Figure 2.1 Registered pulse shapes resulting in coincidence summing [6]

The combined output pulse (coincidence) is undesirable because it causes counts to be lost from both full-energy peaks in the spectrum. If both gamma-rays arriving at the detector within the resolving time of the amplifier were fully absorbed and contribute to their respective full-energy peaks, the coincidence will result in the loss of one count from each peak and the appearance of a count somewhere else in the spectrum. This will create many difficulties in achieving a valid efficiency calibration for close geometry measurements. This problem is not a new one but it has been largely ignored in practice. The problems caused by true coincidence summing (TCS) are illustrated in the calibration curves for a 45% HPGe detector in Figure 2.2. These were derived using Eu-152 near point sources of moderate activity such that the count rate in each case was about 7700 cps. The lower curve is measured with the source at 115 mm from the detector and is smooth and consistent and is apparently satisfactory. The upper curve, measured with the source on the detector cap, is not at all satisfactory. The points do not lie on an orderly line and it would be difficult to draw an acceptable curve through them. The reason for this dramatic difference is due to TCS.

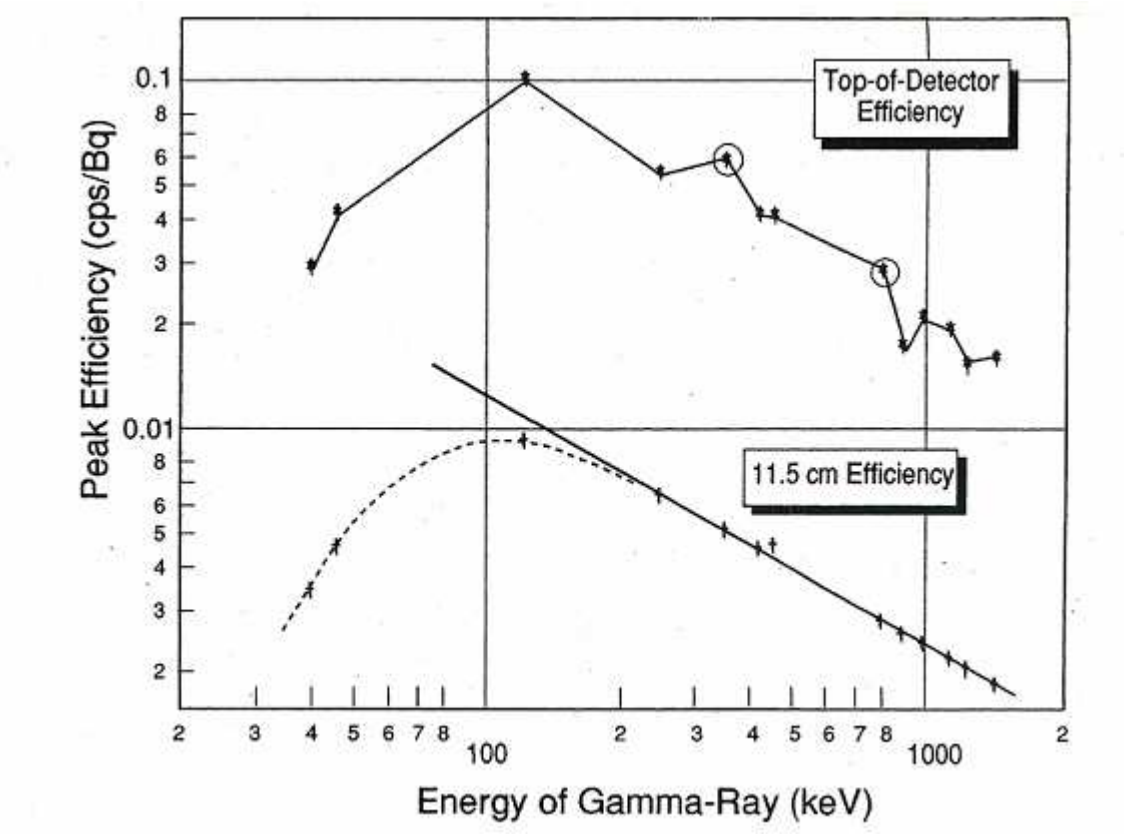

Figure 2.2 Efficiency curves on top of and at 115 mm from the detector end cap using Eu-152 [7]

2.2 The Origin of Summing

A simplified decay scheme for Eu-152 is depicted in Figure-2.3. There are two possible modes of decay for the atoms of this nuclide; they can either emit β^- particle and form Gd-152 or, more likely (72.08% of events), can capture electron to form Sm-152. For both modes of decay, the daughter nucleus eventually de-excits by emitting a number of gamma-rays in any of the decays schemes. Moreover, the electron capture decay to Sm-152 is to be coupled with the emission of Sm X-rays.

The individual nuclear levels have short lifetimes, which are much shorter than the resolving time of the gamma spectrometer system. Each disintegration of an Eu-152 atom in the source releases a number of gamma-rays, possibly X-rays, simultaneously. For the detector, there is a certain probability that more than one of these will be detected together. In that case, the recorded pulse represents the sum of the energies of the two individual photons. This phenomenon is True coincidence summing (TCS), i.e. it is the summing of two gamma-rays emitted in coincidence.

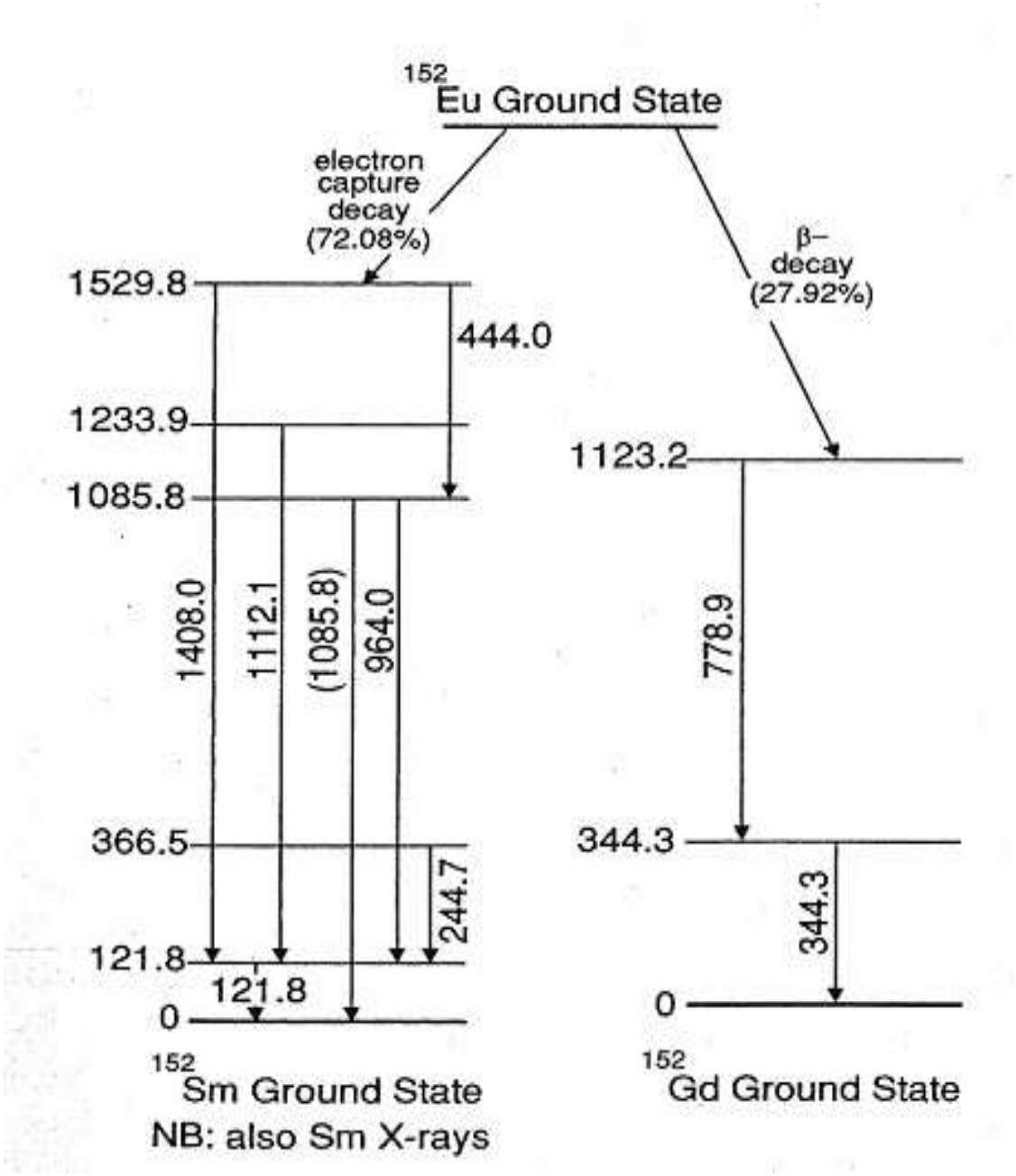

Figure 2.3 Simplified decay scheme of Eu-152 [7]

2.3 Summing and Solid Angle

The degree of TCS is directly related to the probability that two coincident gamma-rays will be detected simultaneously; this is a function of the geometry, of the solid angle suspended at the detector by the source. For the measurements of calibration curves in Figure-2.2, the applied geometrical arrangement is illustrated in Figure 2.4. For the placement of source on the detector cap, the probability, that any gamma ray will reach the detector, is about 45%. Therefore, there is a 20% chance that the two

rays emitted together will both reach the detector. The likelihood that two gamma rays will be detected together, decreases with increasing distance between source and detector. It should be noted that at any source-to-detector distance, there will be some degree of summing. But in practice, depending on the detector size, TCS loses beyond a certain distance are negligible.

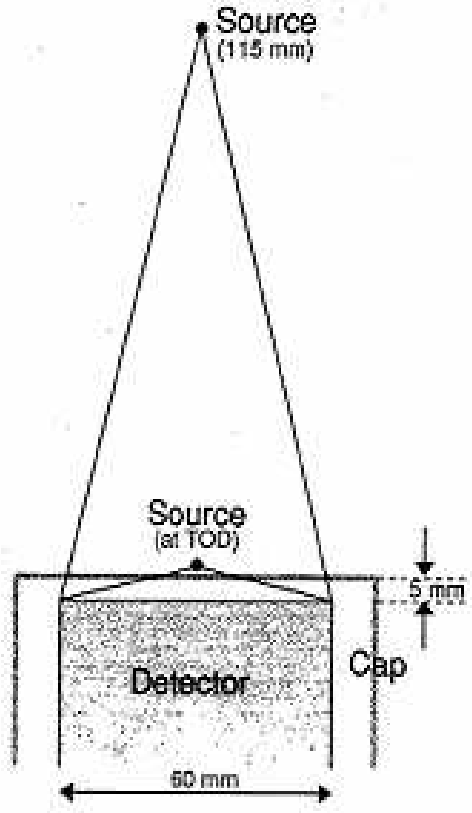

Figure 2.4 Geometrical arrangement used to obtain the data [2]

It should be noted that for a given solid angle, the number of true coincidence summing events per second (but not the ratio of lost/total counts) is proportional to the sample activity.

2.4 Spectral Evidence of Summing

The de-excitation of Sm-152, is likely to produce an X-ray in addition to gamma ray emissions. So X-rays play a prominent role in TCS. For the calibration curves of Figure-2.2, parts of the spectra are shown in Figure-2.5.

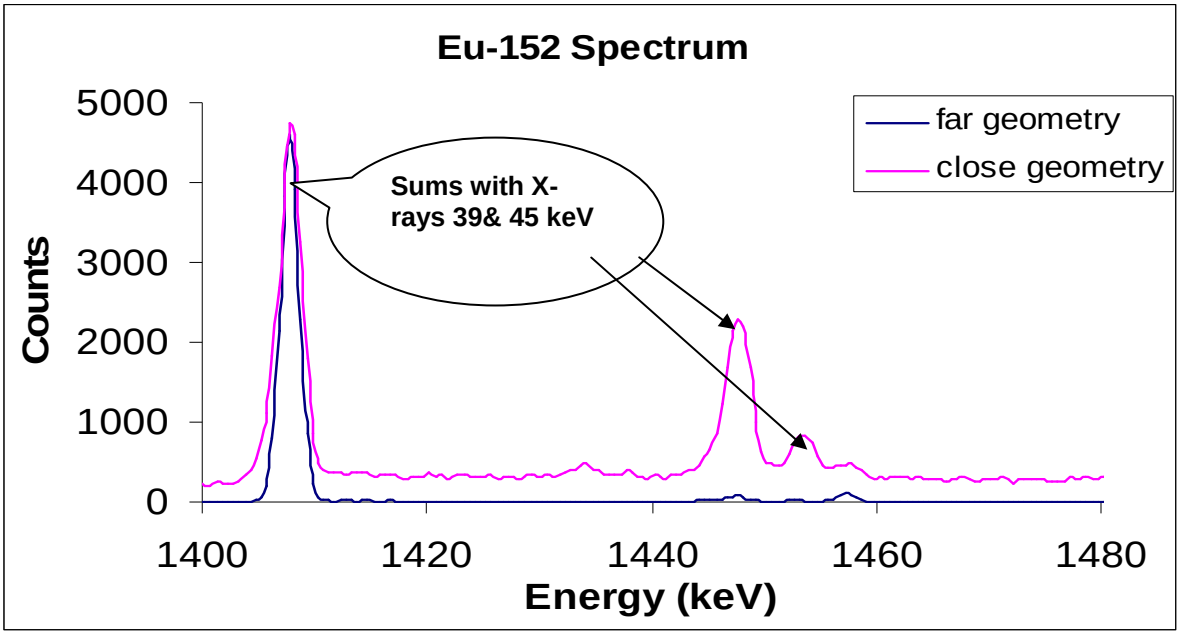

Figure 2.5 Sum peaks above the 1408 keV peak of Eu-152

On comparing the two spectra, pairs of small sum peaks with higher energy than expected, approximately 39.9 and 45.3 keV are observed. This is also clear in low-energy portion of the close geometry spectrum in Table-2.1 which lists close geometry spectrum for coincidence evidences.

Table 2.1 Partial analysis of close geometry spectrum of Eu-152

Energy (keV)	Area (cps)	RSD (%)	Attribution (energies in keV)
39,60	386,0	0.46	Sm K_a X-rays
45,23	109.6	1.00	Sm Kj X-rays
12183	469.2	0.30	
161.62	19.4	3,20	Sum 121.78 + 39.91
167.16	6,0	8,64	Sum 121.78 + 45.4
244.S3	63,8	0,98	
2S4.76	2.6	15.01	Sum 244.70 + 39.91
290,17	1.4	26.54	Sum244.70 + 45-4
296.09	3.0	10.34	
344.44	225.1	0.41	
367.33	10.2	4,85	Sum 121.78 + 244.70
411.28	13,2	270	
444,12	14.4	2,52	■
488,79	1.8	13,51	
564.29	2.6	13,32	Sum 121.78 + 443.97

* Energies here are reported by analysis program [9]

The peaks due to summing with X-rays appear after major gamma ray due to electron capture decay. Additionally, γ-γ coincidences between few Sm-152 high abundance gamma rays can be detected. For the branched Eu-152 decay, radiations originating in different cascades do not indicate summing. e.g. there is no summing between the 121.78 keV and the 344.28 keV gamma-rays or between the Sm branch X-rays and the Gd branch gamma-rays. However, in the spectrum, the (344.28 + 778.90) sum peaks do appear with the beta decay branch.

The sum peaks correspond only to a small fraction of counts lost from main peak because summing can be due to a partially absorbed gamma ray. Since only a small number of gamma rays are fully absorbed, the summing between a full energy peak gamma ray with partially absorbed gamma ray is possible. This can be seen in Figure-2.5, where the level of the background continuum at high-energy side of the peaks is greater than that at the low-energy side in the spectrum affected by TCS. Such coincidences with partially absorbed gamma rays must be taken into account if TCS correction is to be computed.

Furthermore, in case of beta decay, a beta particle and the deexcitation gamma-rays are emitted almost at the same instant, a gamma-ray may sum with the bremsstrahlung produced as the beta particle is slowed down.

2.5 Experimental Evidence of the Need for Corrections

The true coincidence corrections can also be estimated experimentally with sources that emit both coincident and non-coincident photons. Spectra can be recorded for the sources placed both at a distance d_0 from the detector and at the closer distance d chosen for the actual measurements. Analyzing comparatively, the ratio of the peak count rates n(d) and $n(d_0)$ should be a smooth function of the energy for the non-coincident photons. The amount by which the ratios for the coincident photons deviate from this function gives an estimate for the coincidence-summing corrections. An example for this method is given in Figure 2.6 where the typical coincidence-summing correction factors are 60/50 = 1.2 [1]

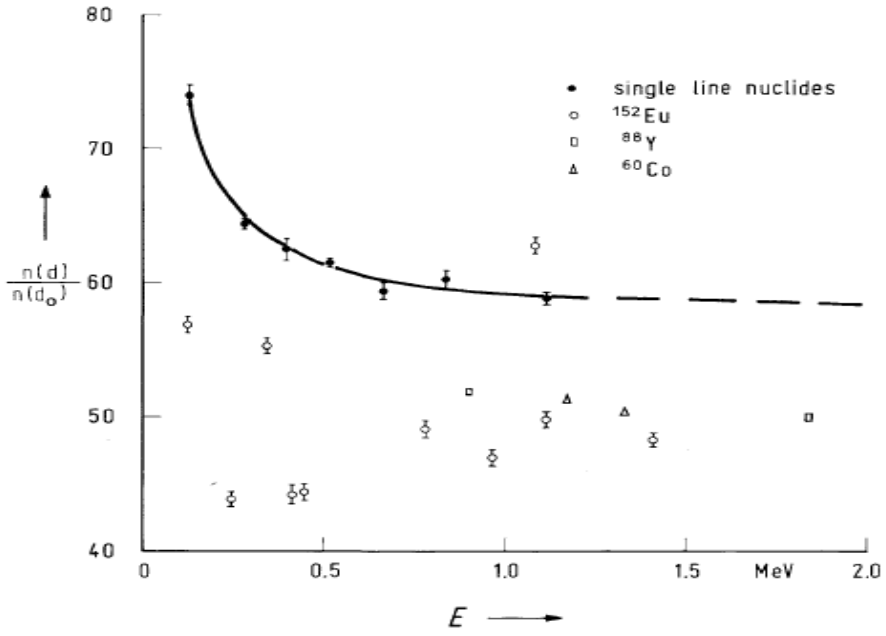

Figure 2.6 Ratio of count rates in the full-energy peaks for a point source positioned at a short distance *d* and a large distance d_0. The solid line has been drawn by hand.[1]

2.6 Validity of Close Geometry Calibration.

It is clear that all the points in the close geometry set (Figure-2.2) are invalid for constructing a calibration curve. Each point represents a valid calibration point for Eu-152 measured on the particular detector, in the particular source geometry on the detector cap and not to any other nuclide. For example, the point representing the 121.8 keV efficiency could not be used to estimate the activity of a Co-57 source through the 122 keV peak area. Co-57 will have its own, different, TCS problems.
The lower curve of Figure-2.2, measured at 115 mm, appears to be more satisfactory. Though this curve is also affected by TCS, the degree of TCS is negligible. For the same source, measured at the same distance on a larger detector, that would not necessarily be the case.

2.7 Summing in Environmental Measurements

The gamma spectrometric measurements of isotopes such as Cs-137 and Cs-134 have been a major preoccupation for many laboratories after the Chernobyl accident (1986). Cs-134 has a relatively complex decay scheme and TCS is almost inevitable given that the environmental sample activities are low and necessarily be measured

close to the detector, often in Marinelli beakers. The extent to which TCS is ignored is best illustrated in Figure 2.7, which shows the results of an intercomparison arranged by the National Physics Laboratory in UK (NPL) in 1989 for the measurements of various radionuclides, including Cs-134, at environmental levels. Out of 58 Cs-134 results reported, only four were within the range expected by the NPL (i.e. within the shaded band in the Figure-2.7.) and in only 11 cases, the true results lied within the 68% confidence limit reported by the laboratory. It is obvious that the majority of the results were low; 64% of results reported were more than 5% below the expected value. The most likely reason for this is that TCS had not been taken into account by the laboratories reporting these results.

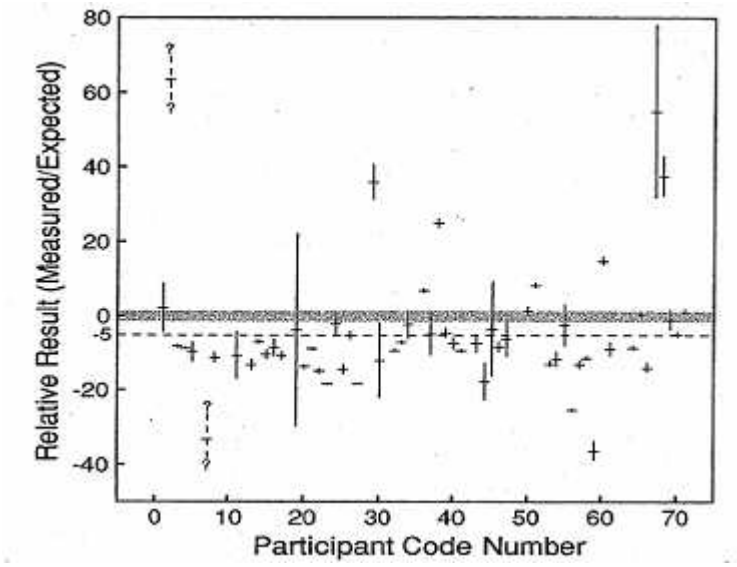

Figure 2.7 Summarized Cs-134 results from the 1989 NPL environmental radioactivity intercomparison exercise.[8]

To achieve accurate results, the true coincidence summing must be taken into account. In fact, further NPL intercomparison exercises in 1990 and 1992 showed similar biases in the Cs-134 results, although slightly smaller on average. Inspite of the growing awareness of TCS, many labroratories do not take it into account.

2.8 Achieving Valid Close Geometry Efficiency Calibrations

A valid efficiency calibration curve can only be measured for close geometry conditions by using radionuclides which do not suffer from TCS. Table-2.2 lists several nuclides which emit only a single gamma-ray and therefore cannot

participate in summing. However, care should be taken with those single gamma-ray nuclides which decay by electron capture (e.g. ^{51}Cr and ^{109}Cd) because a detector with a thin window, especially n-type detectors, may allow significant summing with the X-rays due to the lower absorption in the entrance window.

Table 2.2 Radionuclides suitable for close geometry efficiency calibrations.

Nuclide	Gamma-ray energy (keV)	Nuclide type[a]
^{7}Be	477.6	S
^{40}K	1460.8	S
^{42}K	1524.6	M
^{51}Cr	320.08	SX
^{54}Mn	834.84	SX
^{57}Co	122.06, 136.47	MX
^{64}Cu	1345.8	SX
^{65}Zn	1115.5	SX
^{95}Zr	724.2, 756.7	M
^{95}Nb	765.81	S
^{103}Ru	497.1	S
^{109}Cd	88.03	SX
^{113}Sn	391.70	MX
^{131}I	364.5, 637.0	M
^{137}Cs	661.66	S
^{139}Ce	165.86	S
^{141}Ce	145.4	S
^{144}Ce	133.5	M
^{198}Au	411.80	M
^{203}Hg	279.20	S
^{210}Pb	46.5	S
^{241}Am	59.54	M

S indicates a nuclide emitting a single gamma-ray
M indicates a nuclide for which the gamma-ray mentioned is the major one and has little coincidence summing
X indicates that summing with the accompanying X-rays [9]

There are a number of nuclides which emit multiple gamma-rays though for which summing of the specified gamma-ray, is usually negligible (e.g. Sn-113 and I-131). Other gamma-rays are emitted with such a low abundance that summing, although possible, can be ignored.

The nuclides in the list are convenient to use in practice but it includes some nuclides for which standardized sources may not be readily available and includes

some sources with short half-lives which would not be appropriate for routine calibration. Nevertheless, with an appropriate selection of nuclides it is possible to create a valid close geometry efficiency calibration. The TCS-free single gamma-ray efficiency curve will still be irrelevant to the estimation of the nuclides with complex decay cheme. It needs to be corrected for the summing in the sample measurements

In practice spectrum analysis is constrained by the type of the software used. So it is pertinent to consider how the spectrum analysis program would treat calibration data such as that in Figure-2.2. Most likely it will construct a 'best' but completely invalid fit, perhaps as in Figure-2.8. It is clear that all the points are likely to be lower than they should be and that the true calibration curve should lie above them all.

For comparative analysis, standardized sources are required. The spectrum analysis program calculates results by reference to a calibration curve so, a set of correction factors for each gamma-ray needed to be measured which can be applied to the output from the program. Taking as an example the data in Figure-2.8, the procedure would be;

- Construct an efficiency calibration
- Measure calibrated sources of each the nuclides to be determined, prepared in the standard geometry and of the same density as the samples to be measured.
- Use the computer program to calculate the activity of these sources based upon the estimated calibration. The ratio between measured and actual activities is the correction factor to be applied to the sample measurements.

A fundamental problem arises when standardized reference sources are not available for a particular nuclide; in this case it would be necessary to perform measurements at a large source-to-detector distance using an appropriate TCS-free calibration curve and compare these with the close geometry measurements.

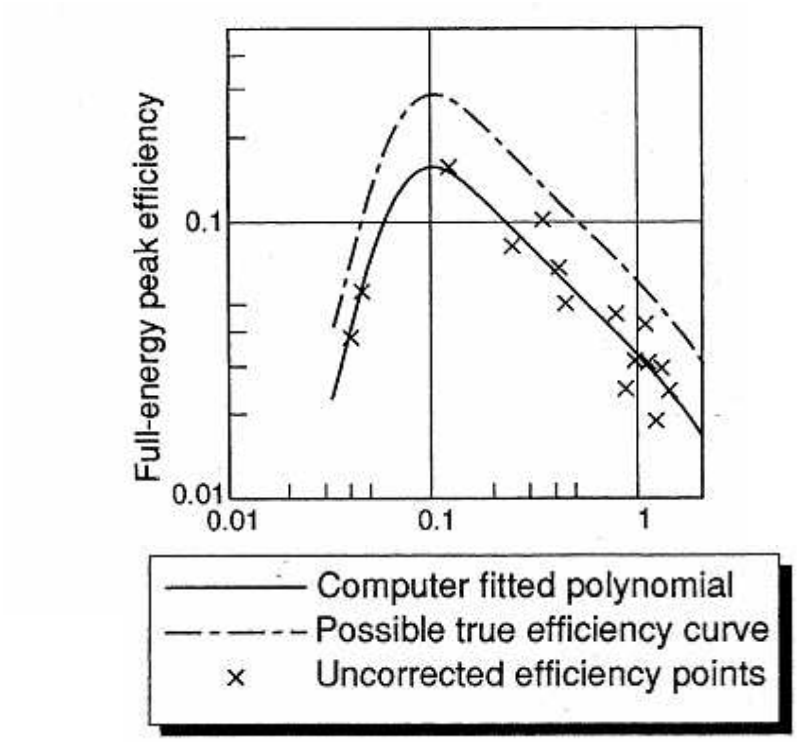

Figure 2.8 The efficiency curve constructed using a 'best fit' computer program [10]

Correction of results after the calculation, while straightforward in principle, is inconvenient for routine operation of a spectrometer system. It is much more acceptable if the final results from the program are correct. This can be achieved by measuring the true coincidence summing correction factors for each gamma-ray to be measured in the samples using comparative measurements or by using the efficiency curve as described above. It is important that these corrections should only be made to the sample measurements, not to the calibration measurements, and separate sample and calibration libraries need to be maintained.

2.9 TCS and Geometry

Table-2.3, lists the peak areas for count rates for Eu-152 as a point source for its distribution of the same activity in sand and in water and measured on the cap of a 45% p-type HPGe detector. The distributed sources had diameter of 13 mm and 20 mm height.

Table 2.3 Count rate of sources of different geometry

Energy (keV)	Peak area (cps)		
	Point	Aqueous	Sand
39.91	386.0	243.1	174.5
45.4	109.6	75.0	58.1
121.78	469.3	325.6	301.0
244.70	63.7	46.4	44.8
344.28	255.1	151.8	139.0
411.13	13.2	9.51	8.62
443.97	14.4	11.0	10.6
778.90	46.6	32.7	30.2
867.39	9.67	7.26	7.23
964.06	35.6	26.4	25.5
1085.84	24.8	16.9	16.3
1112.09	30.4	22.8	22.3
1408.02	38.0	27.42	27.2

All sources have same amount of Eu-152. Aqueous and sand are 13 mm diameter and 20 mm high

Plotting the data graphically as in Figure-2.9 *sketches* scattered peaks areas for the distributed sources relative to the point source. This unexpected scatter of points is not due to the peak area uncertainty, rather it is reminiscent of the scatter on the close geometry calibration. Certain factors lead to such peaks; the Eu-152 in the point source, on the average, is closer to the detector than in the distributed sources. The scatter represents the difference in TCS between the two source geometries. Moreover the difference between the aqueous and sand matrix sources can, in addition to self-absorption, be attributed to the lower TCS in the sand source because of absorption of the Sm X-rays by the sand.

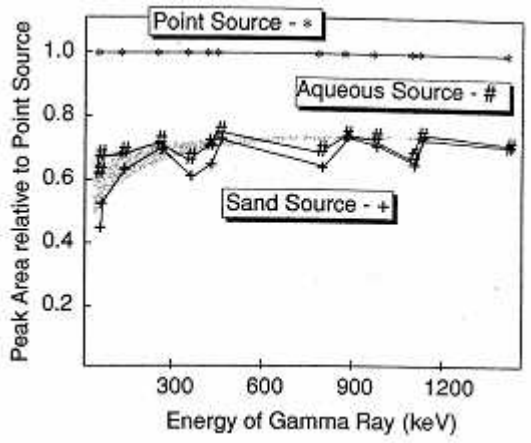

Figure 2.9 Relative peak areas for sources of different geometry and density [10]

The above discussion leads to the conclusion that unless sample and standard (or calibration) sources having identical shape and density, are in identical containers and are measured at the same distance, differences in summing will appear which will not be accounted for by the routine calibration process.

2.10 Mathematical Summing Correction

It is possible, in principle, to correct for TCS errors mathematically. The simplest possible decay scheme in which TCS can be expected, is shown in Figure-2.10. It shows the beta decay to one of two excited states followed by the emission of the three gamma-rays. For the sake of simplification, the internal conversion coefficient for the gamma-rays are all assumed to be zero.

Now, letting the source activity be ***A*** Becquerels, then in the absence of TCS the count rate in the full-energy peak **1** would be:

$$n_1 = Af_1\varepsilon_1 \qquad \textbf{(2.1)}$$

Where, f_1 and ε_1 are the gamma probability and the full-energy peak efficiency respectively for the detection of γ_1. Similar equations would be used to calculate the full-energy peak counts for γ_2 and γ_3.

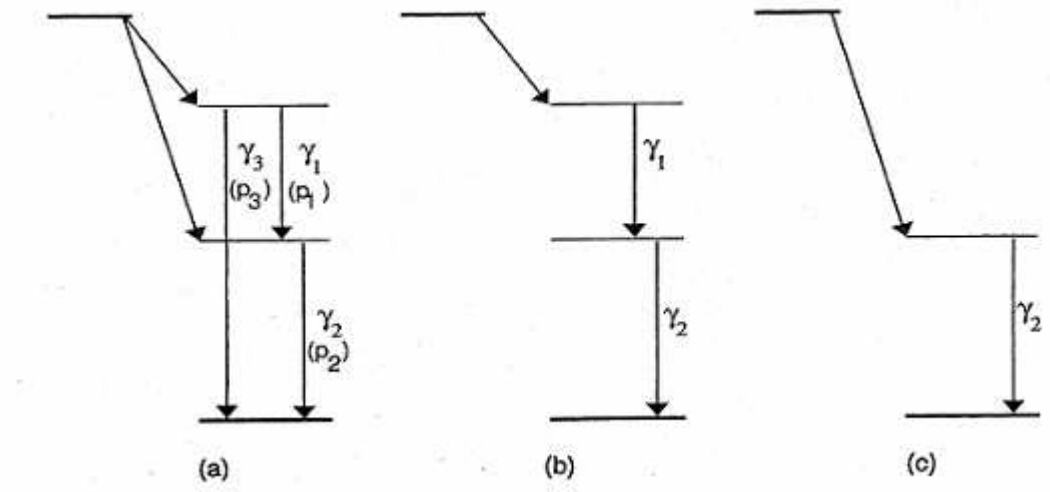

Figure 2.10 Simple illustrative decay scheme liable to true coincidence summing [2]

Now, due to summing of γ_1 with γ_2, counts from the γ_1 peak will be lost. We do not need to consider γ_3, since the de-excitation of the upper level can only give γ_1 or γ_3, not both and only the partial decay scheme in Figure-2.10(b) is needed. The number of counts lost (per second) by summing can be calculated as a product of;

- the number of decaying atoms (A)
- the probability of de-excitation producing $\gamma_1 f p_1$)
- the probability γ_1 of being detected and appearing in the full-energy peak (ε_1)
- the probability of γ_2 being detected and appearing anywhere in the spectrum (ε_{T2})

Therefore all the coincidences whether giving rise to a sum peak count or not, should be taken into consideration and hence the final term uses ε_{T2}, the total efficiency for the detection of γ_2. The net peak area would then be;

$$n_1' = Af_1\varepsilon_1 - Af_1\varepsilon_1\varepsilon_{T2} \qquad \textbf{(2.2)}$$

The ratio n_1/n'_1 would be used to correct for the TCS losses of the γ_1 peak area.

$$C_1 = \frac{n_1}{n'_1} = \frac{1}{1-\varepsilon_{T2}} \qquad \textbf{(2.3)}$$

For γ_2, the slight difference is that, not all gamma-rays emanating from the intermediate energy level are a consequence of the de-excitation from the higher level. Some rays are preceded immediately by the β^- decay and cannot contribute to summing [Figure-2.10 (C)]. The number of summing events is then the product of:

- The number of events giving rise to γ_2**(Af_1)**
- The probability of detection of γ_2 in the in the full-energy peak (ε_2)
- The probability of the detection of γ_1 anywhere in the spectrum (ε_{T1})

And so the net area of peak **2** would be;

$$n_2' = Af_2\varepsilon_2 - Af_1\varepsilon_2\varepsilon_{T1} \qquad \textbf{(2.4)}$$

The ratio n_2/n'_2 would be used to correct for the TCS losses of the γ_2 peak area.

$$C_2 = \frac{n_1}{n'_1} = \frac{1}{1-(f_1/f_2)\varepsilon_{T1}} \qquad \textbf{(2.5)}$$

Every true summing event of completely absorbed gamma rays will produce a count in a peak equivalent to the sum of the energies and so the peak corresponding to the cross-over transition will be increased in area rather decreased. Thus the net count rate would be;

$$n_3' = Ap_3\varepsilon + Ap_1\varepsilon_1\varepsilon_2 \qquad \textbf{(2.6)}$$

The summing correction that would be used to correct for the TCS gains of the γ_3 peak area.

$$C_3 = \frac{n_3}{n'_3} = \frac{1}{1+ f_1\varepsilon_1\varepsilon_2/(f_3\varepsilon_3)} \qquad \textbf{(2.7)}$$

Quite frequently, the cross-over transition probability is small and since the emission probabilities for the normal cascade transition are high, the summing in, can be much greater than the direct emission. Unless taken into account, the error from using peak areas due to this transition would be large.

In general, the internal conversion coefficients are not negligible as were treated in the simplified example above. If the Eu-152 decay scheme would be examined instead, correction for TCS becomes apparent. Then not only every possible γ-γ coincidence must be taken into account but also the possibility of coincidence with the Sm X-ray emitted on the Sm-152 side of the scheme

.

For sources emitting positrons, additional complications arise due to appearance of 511 keV annihilation quanta, in coincidence with gamma-rays from the de-exitation of the daughter nucleus. An analytical solution to this problem is to add a pseudo energy level in which the positron emission leaves the daughter. Then, a conversion coefficient of –0.5 should be assigned to the pseudo-level to take both annihilation

photons into account. Furthermore, the triple coincidences between the most intense gamma-ray and bremsstrahlung coincidences lead to further complications.
In principle, the task is challenging, but if the detailed decay scheme, adequate full-energy peak efficiency data, total efficiency data and complete conversion coefficient data is aavailable, then a mathematical correction is possible.

Table-2.4 lists TCS correction factors for a number of major gamma rays of Eu-152 and Cs-134 calculated by Debertin and Schötzig (1990) using the principle described above. The observations for this case are:

Table 2.4 Examples of calculated TCS correction factors for 4 detector/source arrangements

Energy (keV)	Correction factor (multiplier)			
	A2	B2	A4	C
^{152}Eu				
39.91	1.349	1.559	1.079	—
121.78	1.262	1.648	1.058	1.13
244.70	1.434	2.086	1.088	1.18
344.28	1.146	1.145	1.037	1.07
411.13	1.424	1.432	1.075	—
443.97	1.378	2.373	1.096	1.16
778.90	1.249	1.256	1.045	1.13
964.06	1.249	1.438	1.035	1.10
1085.88*	0.940	1.177	0.992	0.97
1112.09	1.182	1.709	1.035	1.07
1408.02	1.208	1.740	1.038	1.08
^{134}Cs				
604.72	1.252	1.249	1.063	1.13
795.86	1.265	1.258	1.055	1.13
1365.19*	0.839	0.761	0.975	0.85

Detector source geometry
A-12.5% Ge(Li), A2-point source on detector cap, A-4 one litre Marinelli beaker
B-25% n-type HPGe, B2-point source on detector cap
C-30% Ge(Li), 24 mm diameter, 24 mm high source
* indicates cross-over transitions [1]

- The magnitude of the factors is consistent with the scatter in the close geometry curve in Figure 2.2 and with most errors apparent in Figure 2.6.

- The larger Eu-152 factors for the n-type detectors (B2) can be attributed to the extra summing due to lower absorption of the Sm X-ray in this type of the detector.
- The enhancement of the cross-over transitions (1085.88 keV in Eu-152 and 1365.19 keV in Cs-134) is apparent since their correction factors are less than one.
- The larger factors for the point sources (A2, B2) are present as compared to the distributed sources which are effectively closer to the source.

It should be emphasized that these correction factors should only be used only to the particular detector and particular source geometries for which they were calculated. Correction factors for one's own data can only be determined by the actual measurements or by reproducing the reported calculations with the appropriate data for the detector system used. There are a number of well-known computer programs available for calculating TCS, but these are not easily used in conjunction with the commonly used spectrum analysis programs. The thesis work, highlighted in this paper, is meant to find the true coincidence correction factors for the cascade emitting isotopes implemented in the spectrum analysis software, Genie 2000 used for spectroscopic measurements in the Landesmesssetlle für Radioaktivität, Bremen.

3

Implementation of Cascade Corrections in Genie 2000

3.1 Introduction

A high efficiency detector and its optimal measurement geometry is the basic necessity for the following reason:

- To attain highest possible analysis sensitivity for environmental samples
- To reduce the count time to reach a desired precision for an observed activity or to reach lower minimum detectable activity MDAs.

The optimal geometry is attained by positioning the source as close to the detector as possible and selecting the shape of the source most suitable to reach the highest possible efficiency (e.g., Marinelli beaker). With measurements conditions described above, true coincidences may cause systematic errors that can reach levels of more than ten percent for some radionuclides.

As discussed in chapter **2**, the emissions resulting from the majority of decays from a mother nuclide to the ground state of its daughter contain several γ- or **X**-ray photons in cascades within a negligible time frame. This time frame is within the resolution time of the detector system where the detector accumulates all energy deposited in its crystal. Due to this reason, determination of energy of each individual photon emitted by each nuclear level transition is not possible. The detector system can only register the sum effect as the summed energy.

The true coincidence may result in coincidence gaining (summing-in) or coincidence losing (summing-out). The coincidence summing-in effect (S_g probability) increases the observed peak area of the analytical γ-line ($N_{p,g}$), whereas the summing-out effect (L_g probability) decreases the peak area.

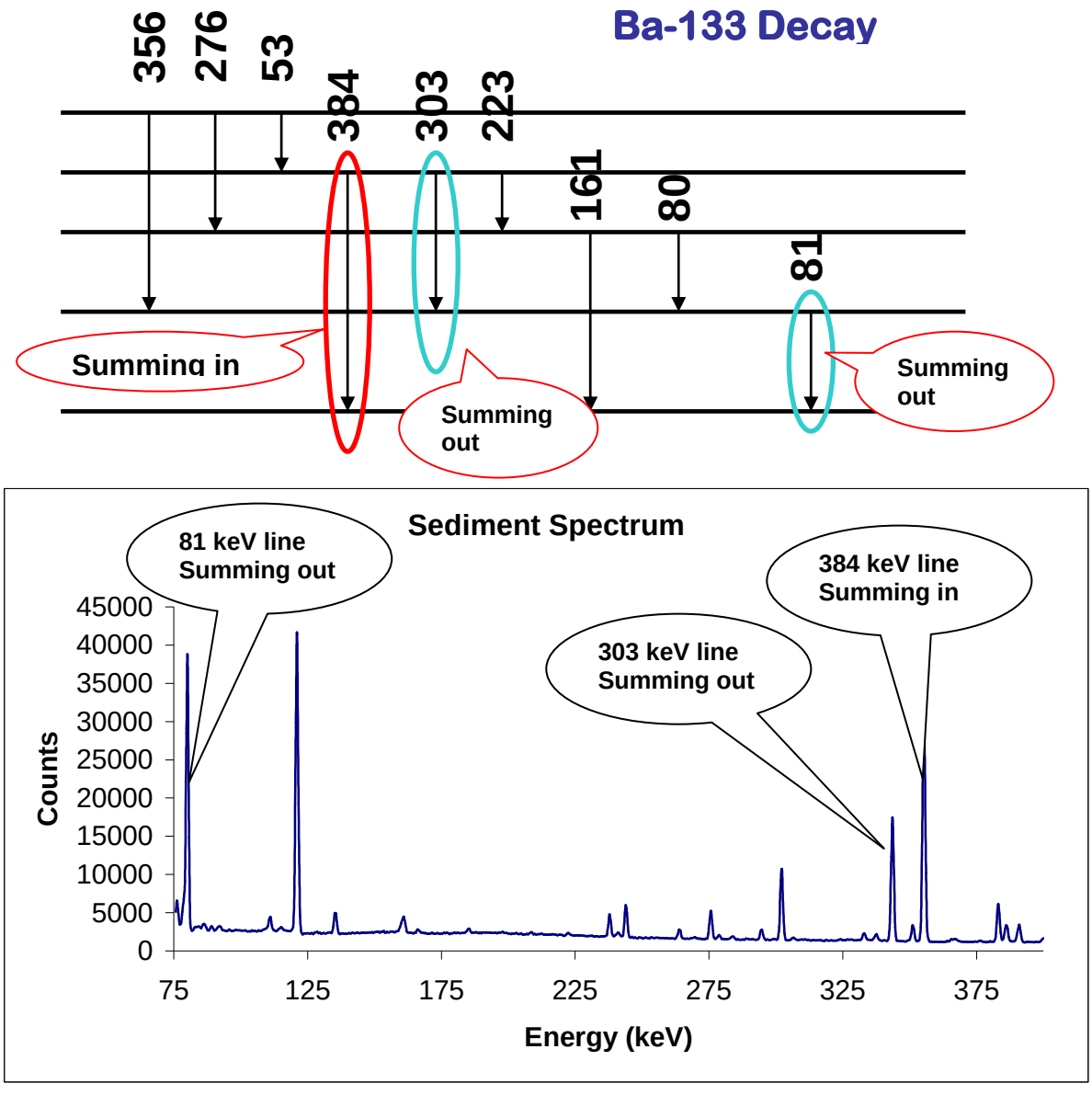

Figure-3.1 The decay scheme and a spectrum of Ba-133 showing the summing-in summing out peaks

For the radionuclide under consideration, the total effect with respect to γ-line g can be described by a coincidence correction factor $\boldsymbol{COI_g}$

$$COIg = (1 - Lg).(1 + Sg) \qquad \textbf{(3.1)}$$

From the observed peak area, the corrected peak area ($\mathbf{N'_{p.g}}$), can be computed using the equation:

$$N'_{p,g} = \frac{N_{p,g}}{COI_g} \qquad \textbf{(3.2)}$$

In case of simple decay schemes, the problem of coincidence correction is well understood for the point sources as can be seen in the section **2.10** (mathematical summing correction) while general formulae for complex decay schemes have been given by ANDREAV et al (1972, 1973)[11,12]. However, for a more general case such as voluminous sources e.g. Marinelli beakers and bottles, the correction for coincidence summing is more complicated due to the complexity of self-absorption and the subsequent cascade summing with partial peak energies, and the formulae given in section **2.10** are no longer valid.

3.2 Estimation of True Coincidence Corrections for Voluminous Sources

The coincidence summing depends on the position within the source volume. To calculate summing correction for voluminous sources the quantities **ε** and $\boldsymbol{\varepsilon_t}$ (defined for the whole source) become useless due to the contribution of the individual source volume elements to the peak areas. The summing effects should therefore be calculated for each volume element ***dV*** from the full-energy peak efficiency **ε(r)** and the total efficiency $\boldsymbol{\varepsilon_t(r)}$ for the specific position r of ***dV.*** So equation **(2.3)** is replaced by

$$1/C_1 = 1 - \int \varepsilon_1(r)\varepsilon_{t2}(r)dV / \int \varepsilon_1(r)dV. \qquad \textbf{(3.3)}$$

Similarly, $\boldsymbol{\varepsilon_{t1}}$ in eq. **(2.5)** is replaced by

$$\int \varepsilon_2(r)\varepsilon_{t1}(r)dV \Big/ \int \varepsilon_2(r)dV \qquad \textbf{(3.5)}$$

and $\varepsilon_1 \varepsilon_2 / \varepsilon_3$ in eq. **(2.7)** by

$$\frac{\int \varepsilon_1(r)\varepsilon_2(r)dV}{\int \varepsilon_3(r)dV} \qquad \textbf{(3.6)}$$

The peak and total efficiencies determination as a function of **r** as well as the energy is tedious.

A summing effect estimation of these coincidences involves direct computation of the effect by means of integration of a function comprising experimentally obtained detection efficiency for the place around the detector[13] while taking into account the sample`s chemical composition and the container´s. The voluminous source is first divided into a large number of equal volumes subsources. The true coincidence correction factor at each of these point locations is calculated and then integrated to determine the overall correction factor for the entire source. In practice, the peak-to-total (P/T) calibration can be used for such integration; also the P/T-ratio for the given energy in the working space around the detector may be considered a constant value[17]. It has been demonstrated that such an approach works quite well for HPGe detectors with the relative efficiency up to 60 % [13].

The influence of angular correlation is assumed to be negligible.

3.3 Peak-To-Total (P/T) Ratios

The P/T ratio is the ratio of the net count in the main peak of the nuclide to the total counts obtained in the spectrum (with background subtraction applied). It is difficult to obtain the exact P/T ratio at each point location (subsource) inside the source volume. Earlier studies[5] have demonstrated that the P/T ratios are weakly dependent on the source-detector distance and considered constant around the detector. The P/T ratios at various points on the top and side of the detector end cap have been measured showing that any small variation in the P/T ratio as a function of source

position will not have a significant impact on the final cascade summing correction factor[6]. The P/T calibration measurements can be performed using a series of individual point sources of nuclides that emit only one gamma ray located at a given source-detector distance since the P/T calibration curve is a property of the detector and not the sample geometry.

Table 3.1 Measured Computed P/T ratios for detector 3 at different geometries

Energy (keV)	P/T ratio at 11cm	Error (%)	P/T ratio at 6cm	Error (%)
59.6	0.506	0.612	0.517	0.612
88	0.816	0.690	0.829	1.239
121.97	0.779	0.158	0.797	0.22
391.46	0.336	0.323	0.352	0.513
661.67	0.244	0.256	0.267	0.172
835.19	0.237	0.419	0.246	0.373
1115.68	0.199	0.143	0.208	0.111

Knowing the P/T ratios for a detector and the total efficiency ε_t at a given gamma ray energy and point inside a sample, the full peak efficiency ε_p at these point can be computed according

$$\varepsilon_t = \frac{\varepsilon_p}{P/T} \qquad \textbf{(3.7)}$$

3.4 Cascade Correction Theory

A discussion about the computation of true coincidence correction for voluminous sources can be based on the work of V.P. Kolotov et al[13]. Based on FEP (full energy peak) measurement, for a certain emitted gamma ray “g”, the activity of a radionuclide, can be written as follows.

$$A = \frac{N_{p,g}}{\varepsilon_g . f_g} \qquad \textbf{(3.8)}$$

For equation **(3.8)**;

$\mathbf{N_{p,g}}$ = measured full energy peak count rate of the gamma line g,

$\boldsymbol{\varepsilon_g}$ = full energy peak efficiency of the whole source, and

$\mathbf{f_g}$ =yield of the gamma line.

As the voluminous source consists of “n” subsources of equal volumes. So the activity of the ith subsource is given by,

$$A_i = \frac{N_{p,g}}{e_g . f_g . n} \qquad \textbf{(3.9)}$$

Each subsource ``i´´ contributes to the measured count rate that is given by,

$$N_{(p,g)i} = A_i . f_g . \varepsilon_{g,i} \qquad \textbf{(3.10)}$$

Here;

$\mathbf{A_i}$ = activity of the ith subsource, and

$\boldsymbol{\varepsilon_{g,I}}$ = full energy peak efficiency of the ith subsource.

To determine partial count rate due to the subsource ´´i``, substitution for $\mathbf{A_i}$ from Equation **(3.9)** results in,

$$N_{(p,g)i} = \frac{(N_{p,g} . \varepsilon_{g,i})}{(\varepsilon_g . n)} \qquad \textbf{(3.11)}$$

If the peak count rate for each subsource is known, and the peak efficiencies and P/T ratios for each gamma line within a given subsource are assumed to be constant, then the coincidence correction ($\mathbf{COI_{g,i}}$) for each subsource can be computed. Consequently the correction for the whole source is obtained by summation.

$$N'_{p,g} = \sum_{i=1}^{n} \frac{N_{p,g} . \varepsilon_{g,i}}{\varepsilon_g . n . COI_{g,i}} = \frac{N_{p,g}}{\varepsilon_g . n} \sum_{i=1}^{n} \frac{\varepsilon_{g,i}}{COI_{g,i}} \qquad \textbf{(3.12)}$$

Where, $\mathbf{N'_{p,g}}$ = peak count rate corrected for cascade summing or true coincidence effects.

Hence, for the voluminous source, the overall true coincidence correction is,

$$COI_g = \frac{N_{p,g}}{N'_{p,g}} \qquad \textbf{(3.13)}$$

And therefore, from Equation **(3.12)**, the overall correction factor is given by,

$$COI_g = \frac{\varepsilon_g . n}{\sum_{i=1}^{n} \frac{\varepsilon_{g,i}}{COI_{g,i}}} \qquad \textbf{(3.14)}$$

For an infinitesimally small subsource volume, the summation in equation **(3.14)** can be replaced by volume integration

$$COI_g = \frac{\varepsilon_g}{\iiint_V \frac{\varepsilon_{g,(xyz)}}{COI_{g,(xyz)}} dxdydz} \qquad \textbf{(3.15)}$$

where

$$\varepsilon_g = \iiint_V \varepsilon_{g,(xyz)} dxdydz \qquad \textbf{(3.16)}$$

For each subsource of the voluminous source, the peak efficiency $\boldsymbol{\varepsilon_{g,i}}$ is calculated using Canberra LabSOCS methodology. This method implies mathematical techniques for the full energy peak efficiency computation of a Germanium detector for any source geometry. LabSOCS calibration software is an option of the application software packages available for Gene 2000 spectroscopy platform. Genie 2000 program is efficiency-curved based, used in the Landesmessstelle für Radioaktivität Bremen for environmental and low-level γ-ray spectrometry.

3.5 Overview of Genie 2000 Gamma Analysis Software

Genie 2000 possess a set of capabilities for spectral analysis and acquisition from Multichannel Analyzers (MCAs). It performs MCA control, spectral display and manipulation, basic spectrum analysis and reporting. Moreover it has options for

comprehensive spectrum analysis for alpha and gamma spectroscopy and quality assurance.

Genie 2000 Basic Spectroscopy Software

Description

For data acquisition, display and analysis in personal computers, Genie 2000 Basic Spectroscopy Software (S500) is a multipurpose environment, which is capable to run various independent count procedures for several detectors simultaneously. It has designed-in network support for remote and multiple accesses to acquisition hardware and other resources.

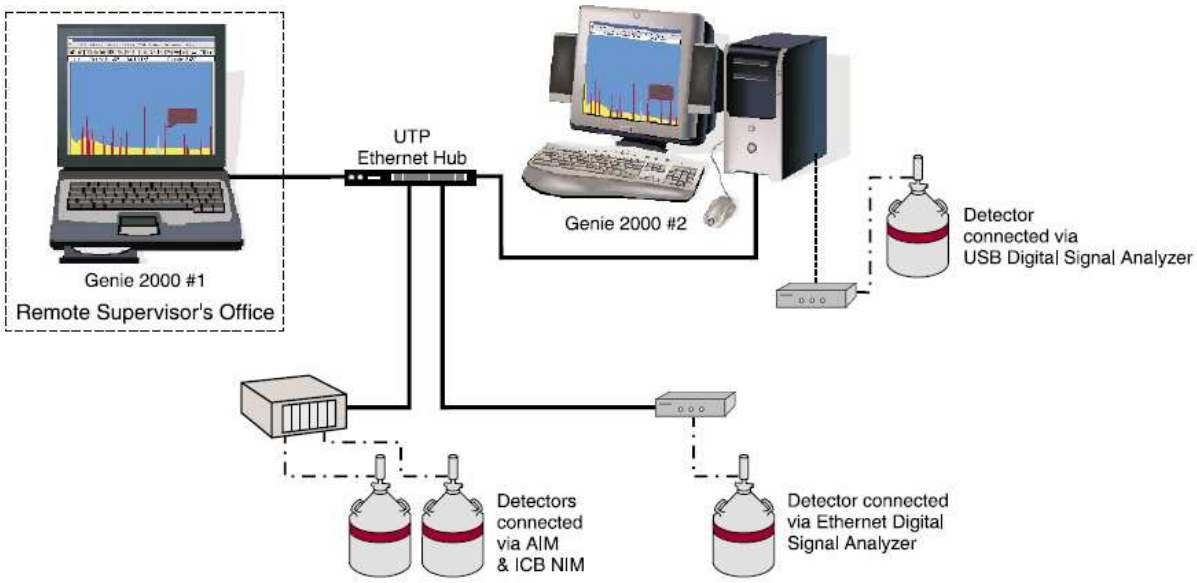

Figure 3.2 Diagram of Multiple Genie 2000 Network.[14]

Spectral Analysis

The Genie 2000 Basic Spectroscopy Software has a set of manually executable base spectroscopic analysis algorithms. These analysis of a spectrum is illustrated below using the following steps:

Complete Calibration Functions.

There are several options for energy (including low-tail and FWHM values) and efficiency calibration and a peak to total calibration can be implied for cascade summing of coincident peaks, these calibrations can be graphically displayed.

Calibrations were done in conjunction with displaying the spectrum in Spectroscopy window. A certificate file (containing energies associated with the nuclide in the standard) was loaded, then energy was selected and after this the peak was selected directly from the spectral display.

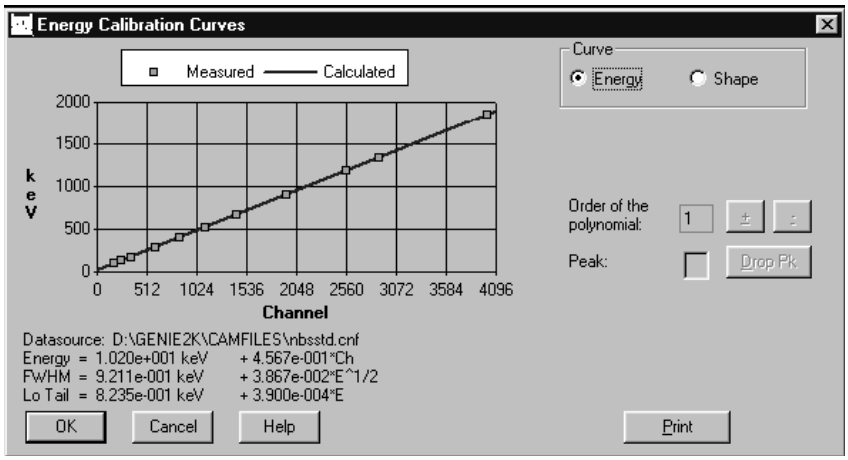

Figure 3.3 A Typical Energy Show Display[15]

The efficiency calibration curve file obtained using standards covering wide range of energies (up to 2 MeV) for each geometry was loaded in which the peak algorithms associated with it to locate and quantify the peaks.The graphical display of the efficiency curve obtained allows to adjust the order of the poynomial of the curve in order to obtain the best fit.

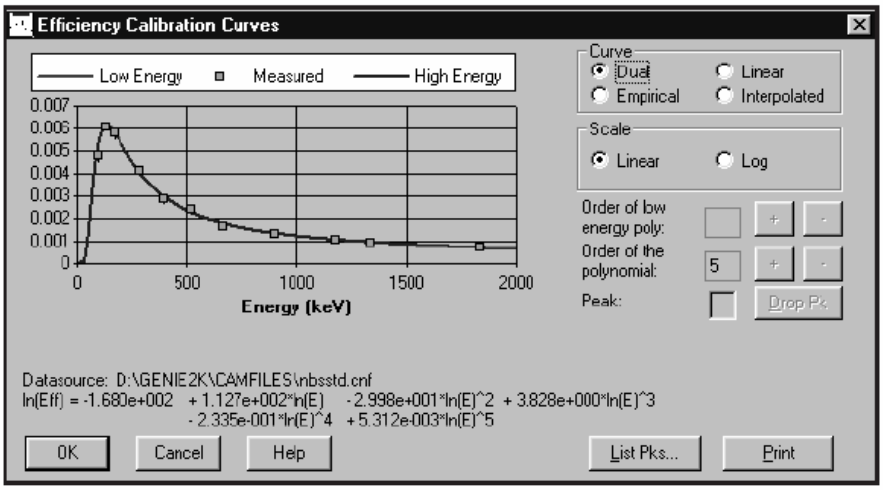

Figure 3.4 Show Efficiency Calibration [15]

Peak Locate and Area

The ‘’Unidentified Second Difference’’ method was selected which searches the spectrum for peaks above specified threshold level and idetifies the centroids of found peaks which can then be used by peak analysis algorithms for peak area calculations.

Tentative Nuclide Identification

An identification of radionuclides for a smple was done by the ``Tentative Nuclide Identification`` (NID) algorithm that looks at each of the peaks established by the Peak Area step of the analysis, and attempts to find a match in the specified nuclide library. The library was created using an editor included within the spectroscopy software in which most of the radioisotopes detected in the laboratory routine and the cascade emitters listed in ``Genie 2000 Coincidence Summing Library``.

The library created is essential for both, the qualitative and quatitative analysis since the NID step takes into account all energy lines of a nuclide entered into the created analysis library with their proper branching ratios, as well as the half life of the nuclide.

The activity of the sample is calculated by

$$A = \frac{N_{Net}}{t.f.\varepsilon} \qquad \textbf{(3.17)}$$

N_{Net} ; the net counts in the peak

t ; the acquisition time of the spectrum

f ; the emission probability of a certain energy line

ε ; the full energy peak efficiency for that energy line

A decay correction is applied to this activity that includes a correction for decay during the acquisition time as well as for decay from the sampling date to the start of the acquisition spectrum.

A complete processing and analysis of gamma spectra is obtained by using Genie 2000 Gamma Analysis Option (S501) and LabSOCS calibration software.

Background subtraction

The background subtraction allows the subtraction of the environmental background (emitted from the walls of the laboratory). A background spectrum is periodically obtained for the laboratory routine work, the spectrum mustmbe analysed separately for its peak locations and associated areas.

Geometry composer

An accurate description of the counting geometry for each sample was created including the detector properties, sample dimensions and densities and distances between the detector and the sample. Knowing these properties is essential for the Cascade Summing Correction factors. The description of the geometries used in the laboratory routine created will be presented in chapter 4.

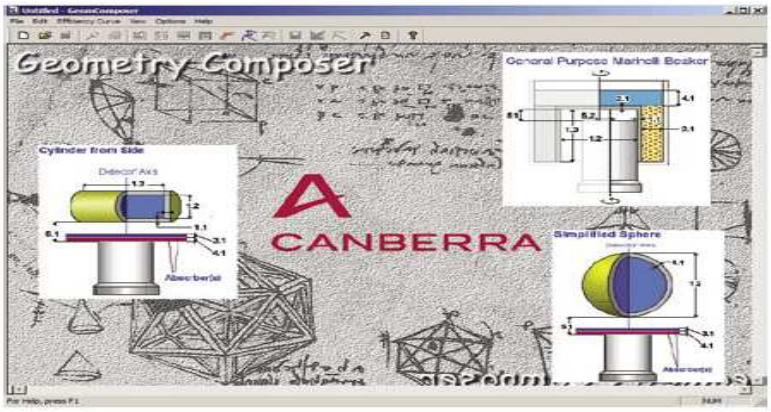

Figure 3.4 Geometry Composer [16]

Minimum Detectable Activity (MDA) calculations

The Minimum Detectable Activity (MDA) was determined based on the detection limit for a given measurement situation (sample's geometry and density). The detection limit, essential to report for environmental measurements , is defined by Currie[17] as the smallest net signal that can be reliably quantified. This is significant for this work since the nuclides that emit gamma rays in a cascade, the net signal will be affected by losses or gains due to cascade summing. Therefore, the cascade correction has to be applied to the Detection Limit, and hence the MDA. Moreover the cascade correction factors were obtained using the MDA of the cascade isotopes as explained in chapter 4.

True Coincidence (Cascade) Summing Correction

This correction was done in NID step to correct against the loss or gain of an observable peak area as a function of nuclide decay scheme and geometry. It can also be applied to correct the full energy peak curve. The true coincidence summing

correction uses LabSOCS technology to precisely describe the sample detector geometry.

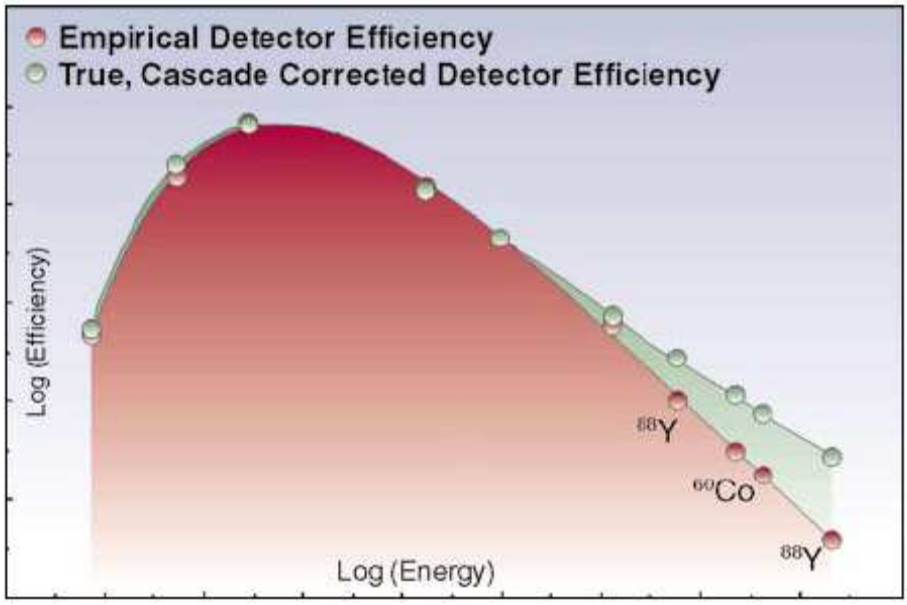

Figure 3.5 Comparison of Cascade Corrected to Empirical Efficiency. [15]

The LabSOCS (Laboratory Sourceless Calibration Software) is a mathematical efficiency calibration software for Germanium gamma sample assay in the laboratory that eliminates the need for radioactive sources for efficiency calibration which saves money and time. It gives the ability to produce accurate quantitative gamma assays of any sample type and size by combining the detector characterization produced with the MCNP modeling code, mathematical geometry templates, and a few physical sample parameters (Figure 4.3).

LabSOCS Calibration also saves time and labor. Instead of week's long traditional process of radioactive source procurement, standards preparation, and long calibration counts.

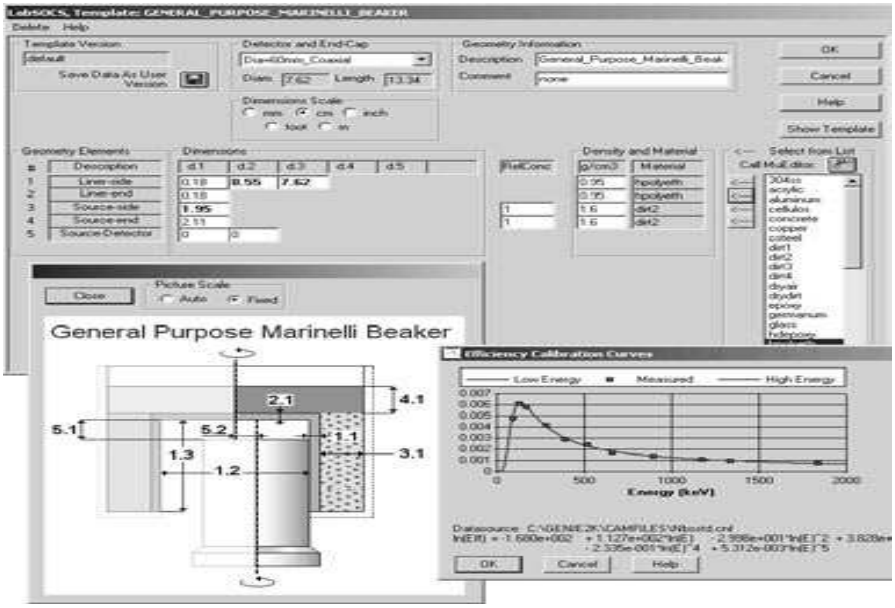

Figure 3.6 LabSOCS Calibration Software is launched, used for data entry, and then generates the Efficiency Calibration Curve[16].

4

Results, Validations and Discussions

4.1 Introduction

The true cascade summing correction for voluminous source are computed using equation **(3.14)** that requires the values of the peak efficiencies ($\varepsilon_{(g)x,y,z}$) inside the source. The values of the cascade corrections for each point ($COI_{(g)x,y,z}$) under integration inside the source are also required, and the computation of these values involves the full peak efficiencies of these points, the decay chain data and the peak-to-total (P/T) ratios. The most important aspect of the used procedure is the necessity to know the P/T ratios for an arbitrary point inside the source. These ratios are determined using point sources of nuclides, which emit one gamma ray of energies covering range upto 2 MeV. The P/T ratios obtained can be used to perform the P/T calibration for the voluminous sample.

Furthermore the description of the samples and container properties and dimensions are needed for this procedure.

The cascade summing correction factors of cascading isotopes frequently detected in the routine analysis for different samples geometries done in the Landesmessstelle für Radioaktivität Bremen, were tabulated for the four detectors in operation in the laboratory. The properties of these detectors are listed in table 4.1.

Table 4.1 Properties of the detectors in operation in LMS

Detectors's Number	Relative Efficiency	Diameter / Length	Resolution at 122MeV (FWHM)	Resolution at 1.33MeV (FWHM)	Geometry
Detector 3	50%	67/61 mm	1.00 keV	1.9 keV	Coaxial
Detector 4	50%	65/62 mm	0.95 keV	2.1 keV	Coaxial
Detector 5	50%	64/60 mm	1.0 keV	2.1 keV	Coaxial
Detector 6	50%	63.5 /63.5 mm	1.0 keV	2.1 keV	Coaxial

Figure 4.1 one of the detectors in the laboratory

4.2 Experimental Work

4.2.1 Peak-to-Total Calibration

The methodology used to correct for cascade summing effects requires the P/T ratios at various point locations within the voluminous source. Since the P/T ratios are

assumed to be constant for detector surroundings, an arbitrary location was selected to obtain these ratios using single line emitters.

4.2.2 Obtaining the Peak-to-Total (P/T) Calibration Curve

A set of uncalibrated point sources (S-PTC P/T Calibration Source Set) was purchased from Canberra Industries for this (Table-4.2). In addition, an Am-241(59.2 keV) source was used.

Table 4.2 S-PTC P/T Calibration Source Set

Nuclide	Energy (keV)	Activity +/- 20%)	Reference Date
Cd-109	88.01	1.0 μ Ci	07/08/2005
Co-57	121.6	1.0 μ Ci	07/08/2005
Sn-113	391.3	1.0 μ Ci	07/08/2005
Cs-137	661.67	1.0 μ Ci	07/08/2005
Mn-54	834.55	1.0 μ Ci	07/08/2005
Zn-65	1115.4	1.0 μ Ci	07/08/2005

The spectra of each nuclide were acquired for the four detectors at a distance 10 cm above the endcap along the axis of the crystal with an acquisition time long enough to have a statistical errror of less than 0.5 % in the main peak.

Since the ambient background in the surroundings of the detector is not negligible, a background spectrum for each detector was acquired. Energy calibration on the point source and background spectra was performed after that.

The peak-to-total ratios at the main peaks (Cd-109, Sn-113) can be inaccurate if the low x-rays that are emitted by these nuclides were not filtered out. For this reason the peak locate and the peak area algorithms were run starting from channel 100 to remove the X-ray counts from the total counts of the spectrum.
The P/T calibration software analyses the point source spectra, performs background corrections and computes the P/T ratios at the gamma ray energies corresponding to the main peaks in the point source spectra.

The P/T values at the main peak energies of the seven nuclides are fitted by a logrithmic function

$$\ln(P/T) = a + b.\ln E_\gamma + c.(\ln E_\gamma)^2 + \frac{d}{E_\gamma^n} \qquad \textbf{(4.1)}$$

The calibration curves for the four detecors were fitted and plotted in the dual mode where 2 low and high energy polynomials cancreated with cross-over energy of 122 keV (Co-57). An order of 2 was used for the high energy polynomial. This provides a linear and predictable extrapolation in the log-log scale.

The figures 4.2 a,b,c and d show the calibration curves obtained for the detectors 3,4,5 and 6 respectively.

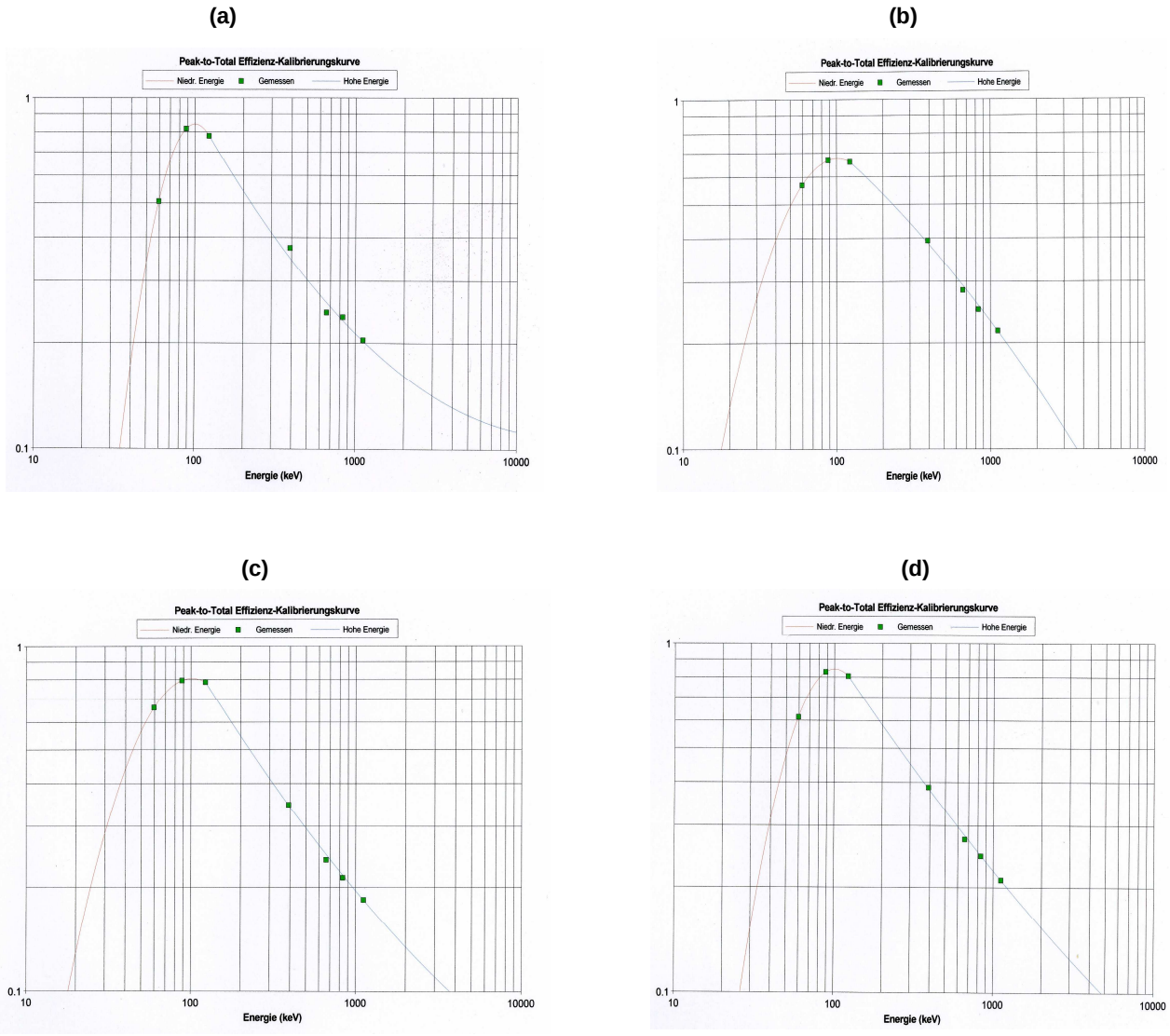

Figure 4.2 The P/T calibration curves for the four detectors in log-log scale

4.2.3 Geometry Description

The proporties of the sample geometries were defined using the Geometry Composer software for HPGe gamma spectroscopy analysis system. Such information is essentail for computing the Cascade Summing Correction factors and include

- The size and shape of the sample and its container.
- The materials and densities from which they are made.
- The type of the detector that will be used for the analysis of this sample.

Table 4.3 lists the sample geometries defined, these geometries are used in the laboratory routine for determining the specific activity of environmental samples.

Geometry	Volume	Density (g/cm^3)
Marinelli Beaker	0.5 & 1 litre	1(water) & 1.5(soil)
Plastic Bottle	0.5 litre	1(water) & 1.5(soil)
Pelletts	5,10 & 20 mm thick 70 mm in diameter	1(water) & 1.5(soil)

Figure4.3 (a) Soil-Wax Pellet

Figure4.3 (b) 1L Marinelli Beaker [18]

Figure4.3 (c) 0.5L plastic bottle

Since detector 3 is characterised for LabSOCS, the geometry descriptions created for that detector were used to buildup full energy peak efficiencies
For the other detectors (4,5 and 6) efficiencies created by using standards in different geometries were used.

4.2.4 CSC Factors Computation

The spectrum analysis steps as explained in chapter 3 were implied to obtain the CSC factor but the detectors should first be calibrated for P/T ratios. Then the corrected values for the specific activities along with the correction factors were obtained

4.3 Results

Tables 4.4, 4.5 and 4.6 list the CSC factors for 1 litre Marinelli beaker (1g/cm^3), 0.5L plastic bottles (1g/cm^3) and 20 mm pellet (1.5 g/cm^3). The factors for all four detectors are listed in Appendix A. Table 4.7 and 4.8 show the comparison between the factors obtained by Genie software and the factors obtained by Korsum software for detectors 4 and 6.

Table 4.4- Cascade correction factors for 1L Marinelli beaker (1g/cm^3)

Nuclide	Energy (keV)	Detector 3	Detector 4	Detector 5	Detector 6
CO-60	1173.23	1,088	1,078	1,092	1,080
	1332,49	1,092	1,078	1,093	1,081
Y-88	898.02	1,081	1,075	1,086	1,000
	1836,01	1,090	1,074		1,074
RH-106	511.70	1,062	1,051	1,060	1,078
AG-110M	657.76	1,238	1,195	1,237	1,000
	706,68	1,317	1,254	1,310	1,203
	884,68	1,236	1,193	1,233	1,267
	937,49	1,227	1,183	1,222	1,201
	1384,3	1,182	1,144	0,118	1,192
BA-133	81	1,141	1,068	1,110	1,100
	302,84	1,025	1,024	1,021	1,100
	356,01	1,019	1,023	1,019	1,020
CS-134	604,72	1,127	1,104	1,124	1,018
	795,86	1,123	1,100	1,119	1,108
EU-152	121.78	1,105	1,108	1,103	1,090
	344,27	1,073	1,061	1,072	1,063
	1085,78	0,978	0,974	0,975	0,974
	1407,95	1,027	1,035	1,029	1,028
TL-208	583,19	1,107	1,104	1,114	1,000
BI-212	727.33	1,030	1,025	1,030	1,000
	1620,5	0,992	0,992	0,993	1,000
BI-214	609.31	1,091	1,077	1,092	1,000
	1120,29	1,101	1,083	1,098	1,000
	1764,49	0,998	0,998	0,999	1,000
AC-228	338.32	1,004	1,002	1,003	1,002
	911,2	1,012	1,010	1,012	1,010
	968,97	1,012	1,010	1,012	1,010
PA-233	312,17	1,001	1,002	1,001	1,001

Table 4.5- Cascade correction factors for 0.5L plastic bottle (1g/cm^3)

Nuclide	Energy (keV)	Detector 3	Detector 4	Detector 5	Detector 6
CO-60	1173.23	1,093	1,094	1,101	1,087
	1332,49	1,094	1,094	1,102	1,088
Y-88	898.02	1,085	1,090	1,095	1,000
	1836,01	1,096	1,090		1,082
RH-106	511.70	1,070	1,062	1,069	1,084
AG-110M	657.76	1,269	1,236	1,277	1,000
	706,68	1,368	1,311	1,370	1,236
	884,68	1,268	1,235	1,270	1,313
	937,49	1,258	1,224	1,255	1,230
	1384,3	1,200	1,175	1,200	1,218
BA-133	81	1,164	1,122	1,137	1,123
	302,84	1,072	1,030	1,027	1,123
	356,01	1,051	1,028	1,026	1,027
CS-134	604,72	1,144	1,125	1,143	1,025
	795,86	1,141	1,122	1,136	1,124
EU-152	121.78	1,121	1,105	1,125	1,109
	344,27	1,083	1,073	1,084	1,073
	1085,78	0,957	0,967	0,970	0,968
	1407,95	1,048	1,044	1,035	1,034
TL-208	583,19	1,117	1,125	1,133	1,000
BI-212	727.33	1,032	1,030	1,033	1,000
	1620,5	0,991	0,991	0,992	1,000
BI-214	609.31	1,099	1,093	1,105	1,000
	1120,29	1,114	1,100	1,109	1,000
	1764,49	0,998	0,998	0,999	1,000
AC-228	338.32	1,002	1,002	1,003	1,002
	911,2	1,015	1,012	1,013	1,011
	968,97	1,013	1,012	1,013	1,011
PA-233	312,17	1,003	1,002	1,002	1,002

Table 4.6- Cascade correction factors for 20mm Pellet (1g/cm^3)

Nuclide	Energy (keV)	Detector 3	Detector 4	Detector 5	Detector 6
CO-60	1173.23	1,160	1,140	1,168	1,143
	1332,49	1,160	1,142	1,171	1,146
Y-88	898.02	1,140	1,137	1,157	1,000
	1836,01	1,170	1,136		1,135
RH-106	511.70	1,110	1,092	1,110	1,142
AG-110M	657.76	1,460	1,375	1,464	1,000
	706,68	1,650	1,504	0,164	1,391
	884,68	1,470	1,372	1,461	1,531
	937,49	1,450	1,353	1,439	1,390
	1384,3	1,360	1,274	1,349	1,371
BA-133	81	1,250	1,190	1,211	1,188
	302,84	1,120	1,048	1,040	1,188
	356,01	1,080	1,045	1,038	1,039
CS-134	604,72	1,240	1,192	1,234	1,037
	795,86	1,240	1,188	1,226	1,201
EU-152	121.78	1,180	1,159	1,188	1,162
	344,27	1,130	1,109	1,131	1,113
	1085,78	0,930	0,949	0,952	0,950
	1407,95	1,080	1,071	1,057	1,056
TL-208	583,19	1,190	1,194	1,213	1,000
BI-212	727.33	1,050	1,044	1,053	1,000
	1620,5	0,985	0,987	0,987	1,000
BI-214	609.31	1,160	1,139	1,169	1,000
	1120,29	1,200	1,153	1,185	1,000
	1764,49	0,997	0,997	0,998	1,000
AC-228	338.32	1,000	1,002	1,005	1,003
	911,2	1,020	1,018	1,021	1,018
	968,97	1,020	1,018	1,021	1,018
PA-233	312,17	1,010	1,003	1,003	1,003

Figure 4.7 Comparison between the factors obtained by Genie and Korsum for detector 4.

Nuclide Energy (keV)	efk 41230 MB_1L_1g/cc	G_41230	efk 42230 MB_1L_1.5g/cc	G_42230	efk 41450 T_5mm_1g/cc	G_41450	efk 41470 T_20mm_1g/cc	G_41470	efk 42470 T_20mm_1.5g/cc	G_42470
CO-60 1173.23	1.071	1.078	1.079	1.076	1.201	1.194	1.125	1.144	1.101	1.140
1332.49	1.074	1.078	1.076	1.076	1.204	1.198	1.127	1.146	1.104	1.142
SE-75 279.54	1.004	1.063	1.002	1.059	1.006	1.189	1.006	1.135	1.005	1.128
Y-88 898.02	1.070	1.075	1.071	1.074	1.206	1.187	1.130	1.139	1.101	1.137
1836.01	1.085	1.074	1.083	1.072	1.213	1.191	1.140	1.140	1.116	1.136
RH-106 511.70	1.053	1.051	1.052	1.049	1.122	1.127	1.081	1.094	1.071	1.092
621.94	1.100	1.089	1.095	1.086	1.230	1.241	1.150	1.173	1.134	1.168
AG-110M 657.76	1.191	1.195	1.192	1.190	1.529	1.535	1.322	1.384	1.268	1.375
763.94	1.198	1.199	1.196	1.193	1.542	1.552	1.330	1.395	1.277	1.384
884.68	1.200	1.193	1.197	1.187	1.535	1.538	1.328	1.383	1.278	1.372
937.49	1.193	1.183	1.190	1.177	1.509	1.513	1.313	1.364	1.268	1.353
BA-133 81	1.147	1.068	1.117	1.098	1.280	1.274	1.197	1.195	1.182	1.190
356.01	1.052	1.023	1.040	1.021	1.113	1.065	1.100	1.048	1.075	1.045
CS-134 604.72	1.108	1.104	1.107	1.101	1.270	1.270	1.172	1.197	1.148	1.192
795.86	1.111	1.100	1.107	1.097	1.263	1.267	1.170	1.193	1.149	1.188

G: for factors obtained by Genie

Figure 4.8 Comparison between the factors obtained by Genie and Korsum for detector 6

Nuclide Energy (keV)	efk 61230 MB_1L_1g/cc	G_61230	efk 62230 MB_1L_1.5g/cc	G_62230	efk 61450 T_5mm_1g/cc	G_61450	efk 62450 T_5mm_1.5g/cc	G_62450	efk 61470 T_20mm_1g/cc	G_61470	efk 62470 T_20mm_1.5g/cc	G_62470
CO-60 1173.23	1.077	1.080	1.076	1.077	1.165	1.198	1.153	1.197	1.165	1.147	1.119	1.143
1332.49	1.078	1.081	1.760	1.078	1.171	1.204	1.154	1.202	1.168	1.150	1.123	1.146
SE-75 279.54	1.002	1.051	1.002	1.048	1.047	1.149	1.027	1.145	1.019	1.108	1.019	1.102
Y-88 898.02	1.076	1.074	1.078	1.073	1.252	1.183	1.203	1.182	1.197	1.137	1.148	1.135
1836.01	1.080	1.078	1.076	1.075	1.278	1.201	1.228	1.198	1.206	1.146	1.162	1.142
AG-110M 657.76	1.192	1.201	1.178	1.195	1.473	1.565	1.453	1.556	1.439	1.401	1.324	1.390
763.94	1.195	1.207	1.182	1.199	1.477	1.575	1.448	1.567	1.443	1.410	1.324	1.399
884.68	1.192	1.201	1.178	1.195	1.473	1.565	1.453	1.556	1.439	1.401	1.324	1.390
937.49	1.184	1.192	1.169	1.185	1.455	1.541	1.439	1.532	1.418	1.383	1.311	1.371
BA-133 356.01	1.026	1.018	1.023	1.017	1.476	1.052	1.350	1.051	1.232	1.039	1.226	1.037
356.01	1.026	1.018	1.023	1.017	1.476	1.052	1.350	1.051	1.232	1.039	1.226	1.037
	1.104	1.108	1.096	1.105	1.243	1.283	1.235	1.279	1.225	1.206	1.171	1.201
795.86	1.103	1.104	1.091	1.100	1.246	1.280	1.237	1.275	1.222	1.202	1.171	1.196

G: for factors obtained by Genie

It should be noted that the factors obtained from the software are shown only for the radioisotopes present in the sample's spectrum and it is impossible to have a sample containing all the cascade emitters. The listed factors are the ratios obtained when the CSC application is implied to that when CSC is not implied

The effect of cascade correction is most evident when applied to high efficiency geometries. Figure 4.4 shows how this factor changes for the Co-60 (1332 keV) and Cs-134 (604 keV) changing with geometries. A progressively decreasing trend in the factors with increase in volume is clearly visible which is due to the decrease of the sample's efficiency.

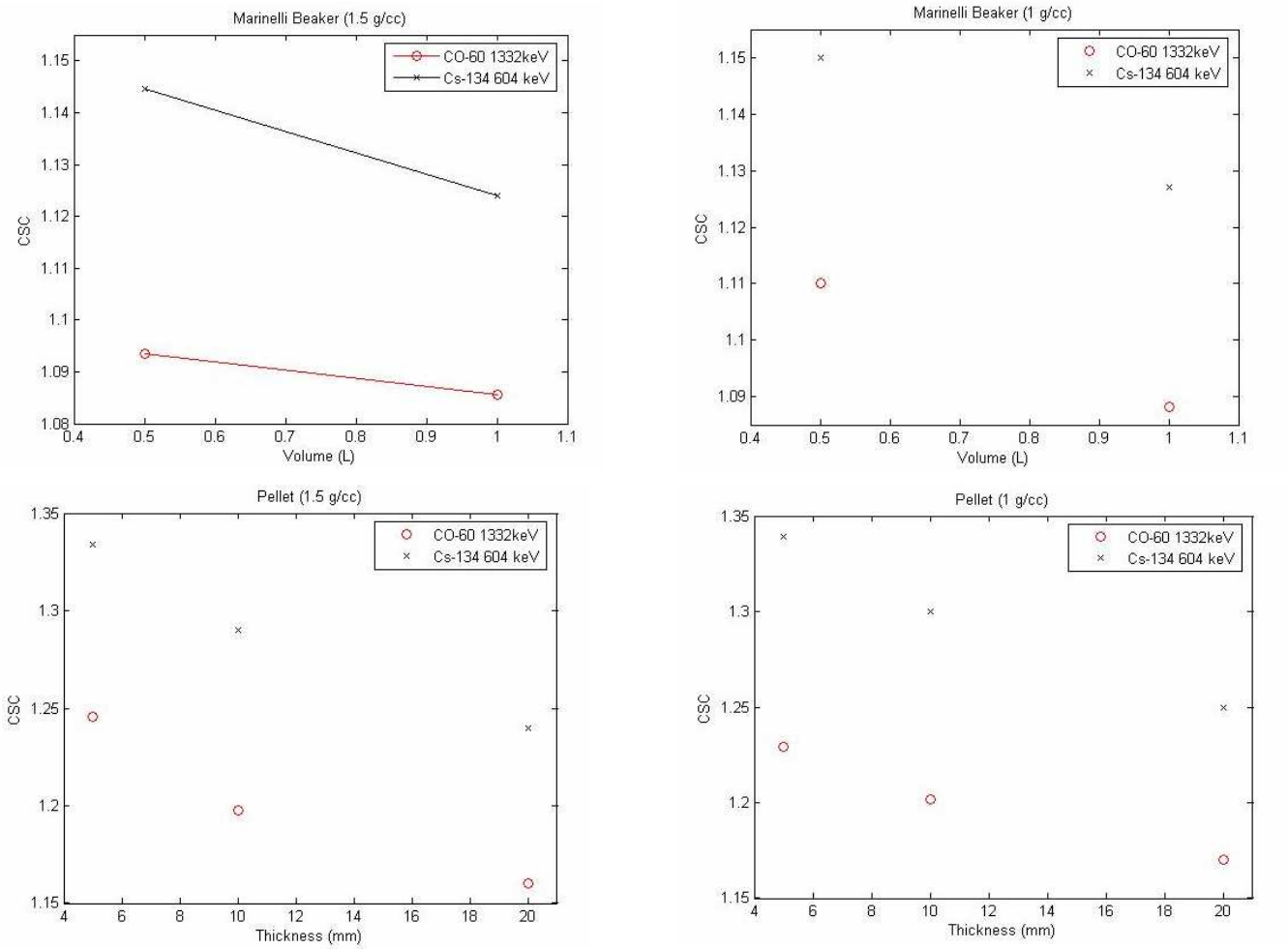

Figure 4.4 The trend of the factors with volume

4.4 Validations and Discussion

To validate the accuracy of the cascade summing correction method, archived spectra of calibrated sources acquired for 0.5,1 liter Marinelli beaker and20 mm thick pellets (1g/cm^3, contains Co-60 and Cs-134) and 20 mm thick sediment pellets (1.5g/cm^3, contains natural and artificial isotopes) for the laboratory intercomparison tests which were performed by the Landesmessstelle für Radioaktivität in 2006 for the BfS and BfG. More measurements were done using calibration standard solution (1g/cm^3 contains Co-60 and Cs-134) for petri dish and 0.5 liter Marinelli beaker geometries.

The measured/certificate activity ratios for these geometries were calculated and shown in the following figures

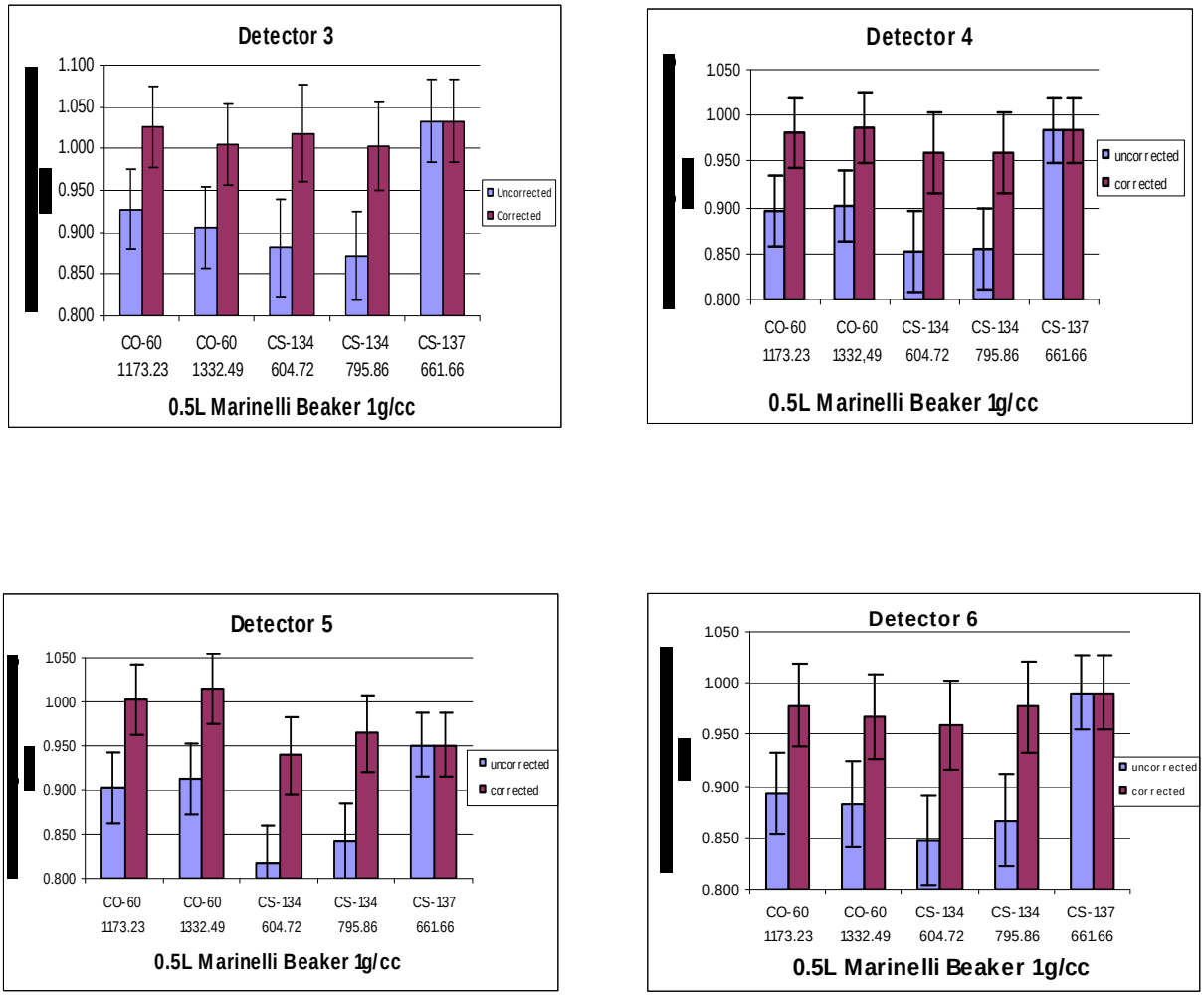

Figure 4.5 (a) The measured/certificate activity ratios for 0.5L Marnelli beaker (1g/cc)

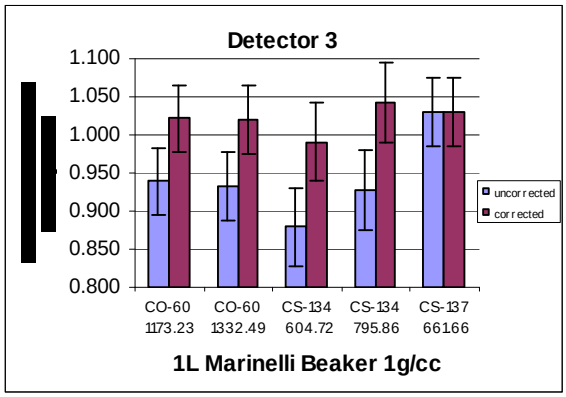

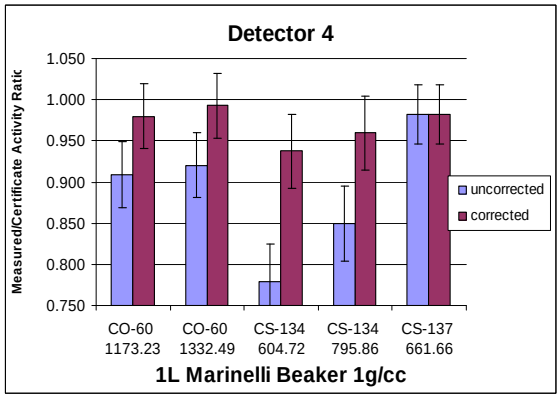

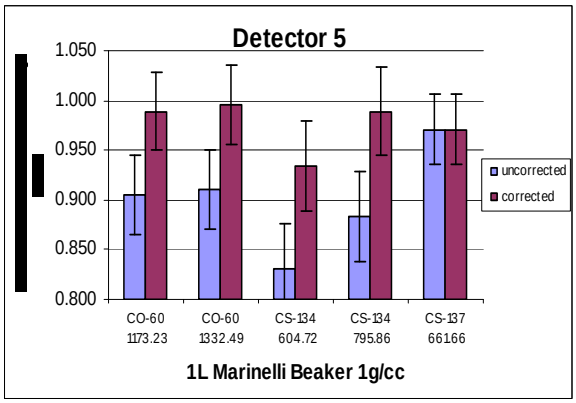

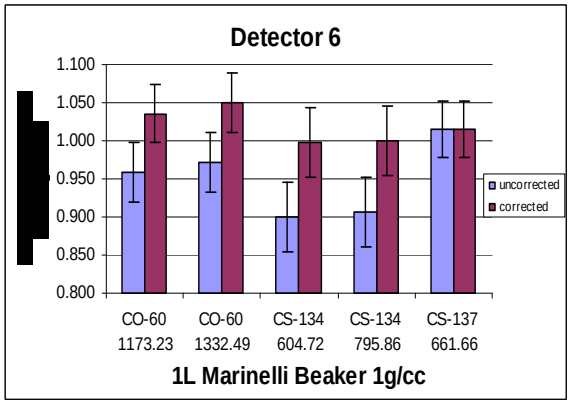

Figure 4.5 (b) The measured/certificate activity ratios for 1L Marnelli beaker (1g/cc)

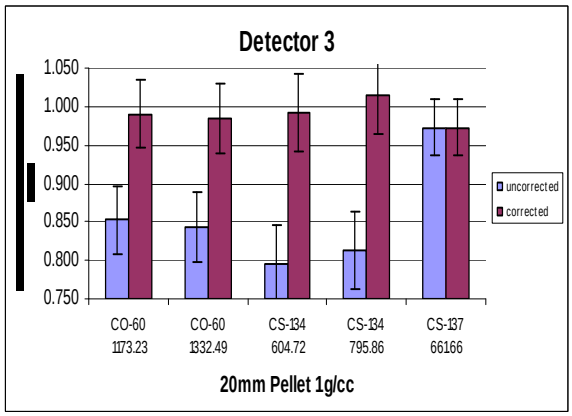

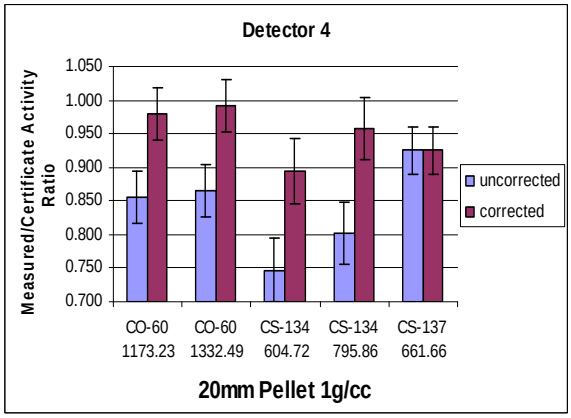

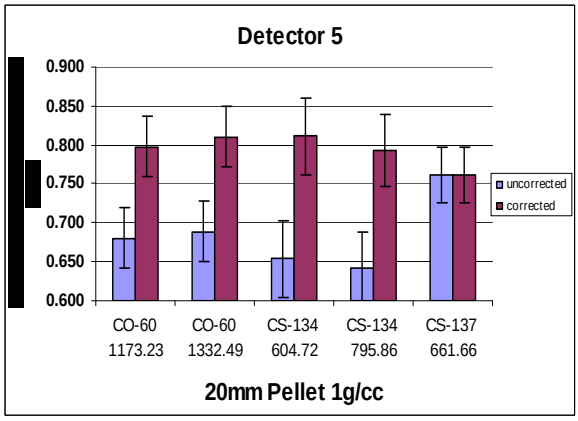

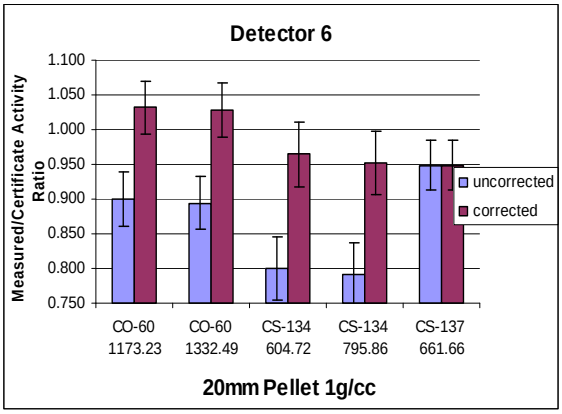

Figure 4.5 (c) The measured/certificate activity ratios for 20mm pellet (1g/cc)

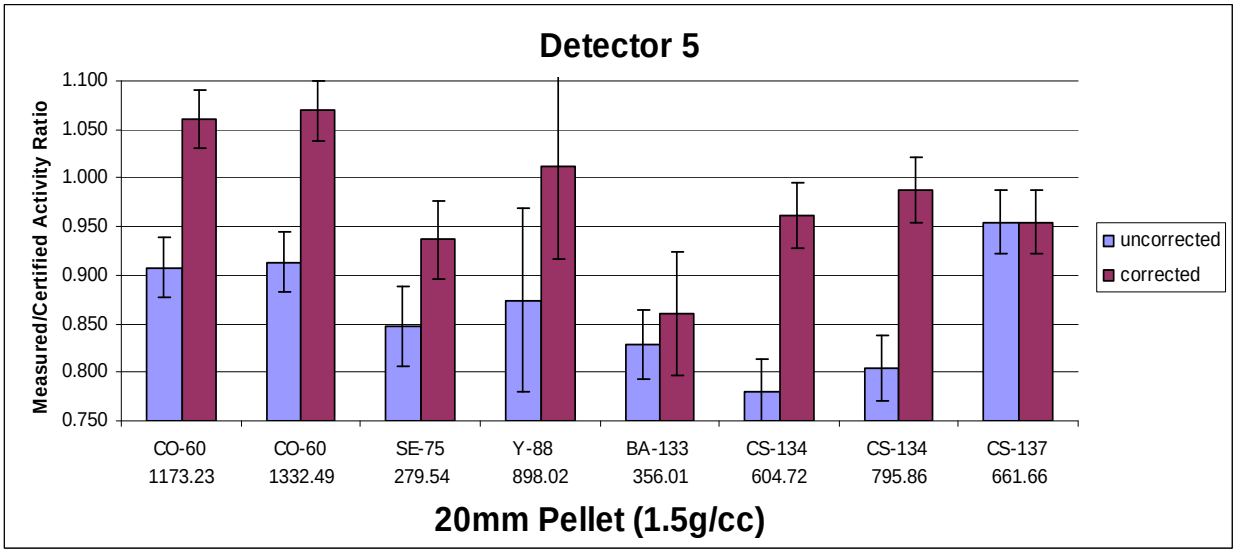

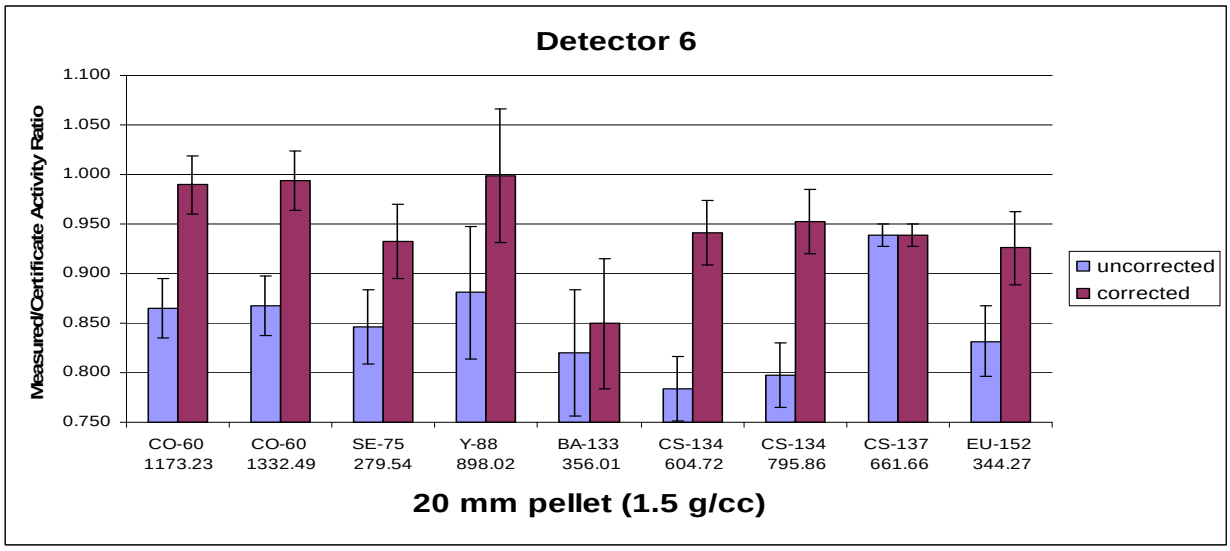

Figure 4.5 (d) The measured/certificate activity ratios for 20mm pellet (1.5g/cc) for artificial nuclides

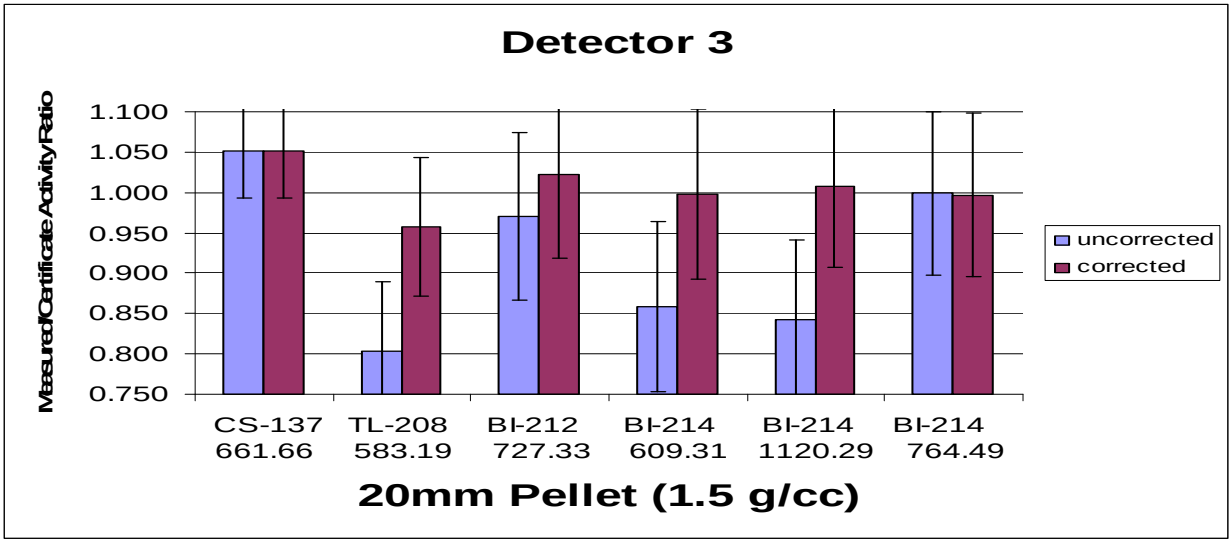

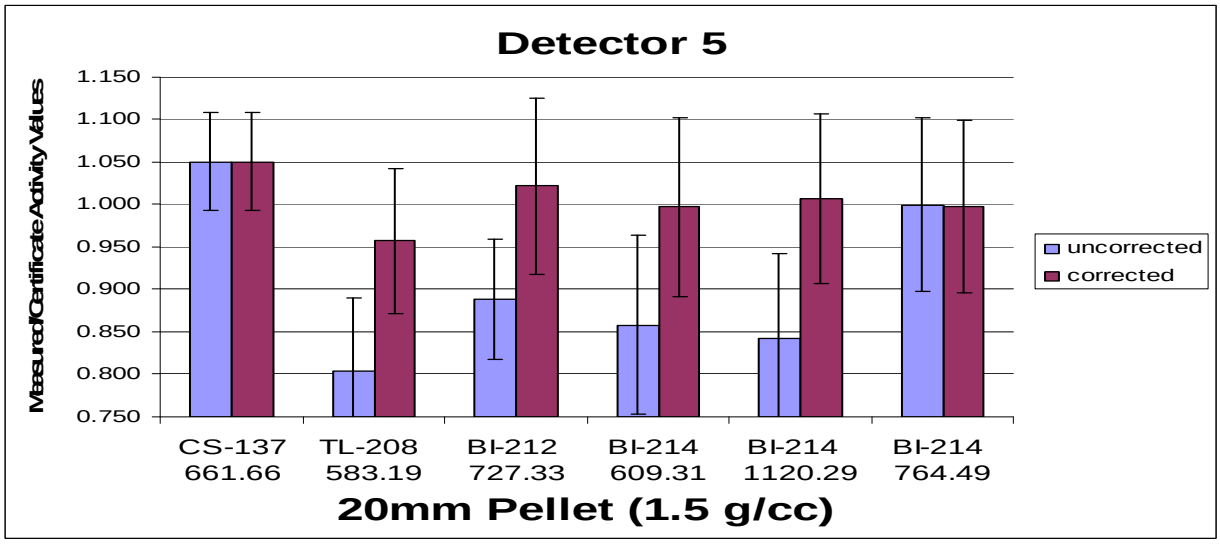

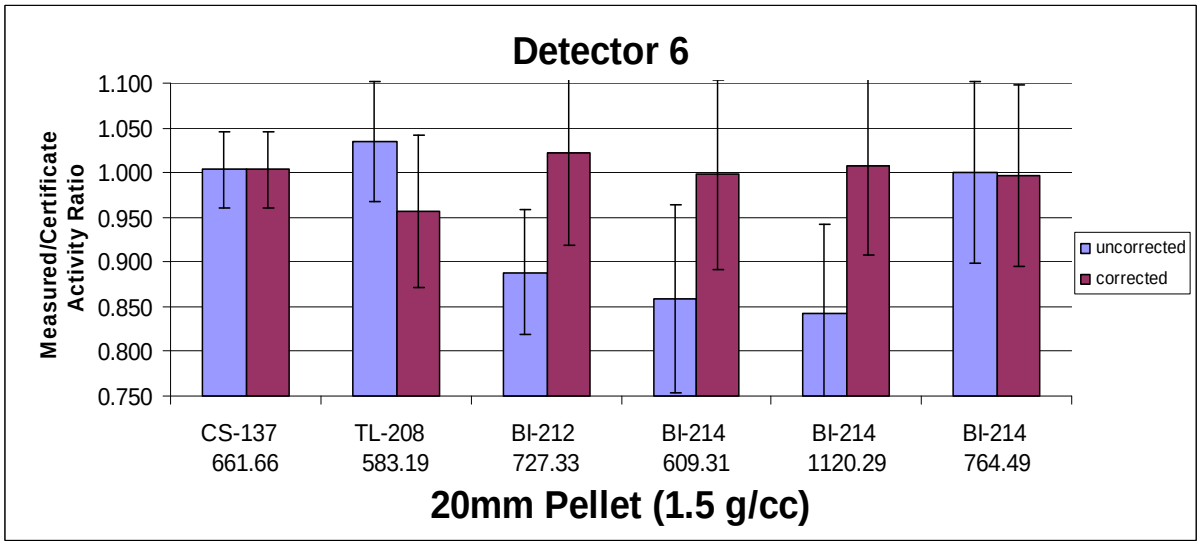

Figure 4.5 (e) The measured/certificate activity ratios for 20mm pellet (1.5 g/cc) for natural isotopes

The sediment sample obtained from BfG was not homogenous that is why 5 pellets were made and measured and the average specific activity was reported. The corrected values presented in Figure 4.5 (e) were compared to the PTB reported value[24] since the intermediate report received by the BfG did not include the certified specific activity of the isotopes but the reported results of the laboratories in that intercomparison test including the PTB

Discussion

The validation figures show the corrected and the uncorrected results separately for the intense lines of the cascade emitters. A quick glance at the corrected values obtained shows that they are improved and are close to the reported certificate values within ±3-5%.

The results shown for detector 5 in the figure 4.5 (c) are considerably deviated from the value of 1. This does not indicate that the correction procedure was not accurate since the corrected values are brought up to values close to that of the Cs-137 isotope within 5%. In this case the spectroscopic system loses part of the signal.

The correction factors obtained by Genie and Korsum soft wares seem to be in good agreement especially for low efficiency geometries and simple decay schemes. The factors for Se-75 and Ag-110m have a discrepancy that reaches 10%. This can be due to the fact that these isotopes have a complex decay scheme ,and the factors used derivate for this procedure were derived considering simple decay schemes.

The specific activity of Cs-137 did not change due to the correction application. The non-cascading Cs-137 isotope was included to confirm the accuracy of the peak efficiency calibration, to show the agreement with the certificate activity and the effect of the correction procedure on the non-cascading isotopes. It is clearly seen that the correction procedure has no effect on the non-cascading isotopes.

The error bars represent the propagated standard deviation of the ratios. These error bars are not only due to cascade correction factors but the factors discussed in chapter 1 including efficiency, electronics.

Based on our verification and validation analysis, the cascade correction factors are estimated to introduce a systematic uncertainty of ±5% (1σ) in the final activity results. The probable reason for any over or under correction in the measured corrected activities could either be the bias in the peak efficiency calibrations or the accuracy of the P/T calibrations. The measured P/T ratio turns out to be sensitive to the presence of scattering materials as the voluminous samples.

The procedure for cascade correction using P/T calibration correction for the characterization of the HPGe detectors for voluminous samples is effective with all corrected line activities for all geometries resulting in one standard deviation of the average non cascading line activities. After applying correction, the errors caused by cascade summing ranging over 20% are typically reduced to 5% or even less. The procedure results in an insignificant change in the measurements considering time where P/T can be used for the whole acquired for the detector since these ratios are properties of the detector and not for a specific geometries. The corrected values can be obtained with a single click.

Appendix A

Detector 3: Marinelli beaker

Nuclide	Energy (keV)	0.5 L (1g/cm^3)	0.5 L (1.5g/cm^3)	1 L (1g/cm^3)	1 L (1.5g/cm^3)
CO-60	1173.23	1,110	1,094	1,088	1,086
	1332,49	1,110	1,094	1,092	1,089
SE-75	121,12		1,168	1,127	1,124
	136		1,171	1,127	1,122
	264,66		1,141	1,084	1,080
	279,54		1,090	1,051	1,049
	400,66		0,633	0,715	0,730
Y-88	898.02	1,100	1,086	1,081	1,079
	1836,01	1,110	1,094	1,090	1,088
RH-106	511.70	1,080	1,071	1,062	1,061
AG-110M	657.76	1,290	1,271	1,238	1,231
	706,68	1,390	1,369	1,317	1,308
	884,68	1,290	1,267	1,236	1,228
	937,49	1,280	1,257	1,227	1,219
	1384,3	1,220	1,197	1,182	1,176
I-131	364,49	1,000	1,000	1,000	1,000
BA-133	81	1,160	1,167	1,141	1,137
	302,84	1,030	1,070	1,025	1,023
	356,01	1,030	1,050	1,019	1,018
CS-134	604,72	1,150	1,145	1,127	1,124
	795,86	1,150	1,140	1,123	1,119
EU-152	121.78	1,120	1,124	1,105	1,104
	344,27	1,090	1,085	1,073	1,072
	1085,78	0,970	0,959	0,978	0,979
	1407,95	1,040	1,045	1,027	1,025
TL-208	583,19	1,130	1,119	1,107	1,105
BI-212	727.33	1,040	1,032	1,030	1,029
	1620,5	0,990	0,992	0,992	0,992
BI-214	609.31	1,110	1,100	1,091	1,089
	1120,29	1,120	1,113	1,101	1,097
	1764,49	0,998	0,998	0,998	0,998
AC-228	338.32	1,000	1,002	1,004	1,004
	911,2	1,020	1,014	1,012	1,012
	968,97	1,010	1,013	1,012	1,012
PA-233	312,17	1,000	1,003	1,001	1,001

Detector 3: Plastic Bottle (0,5L)

Nuclide	Energy (keV)	1g/cm^3	1.5g/cm^3
CO-60	1173.23	1,093	1,090
	1332,49	1,094	1,090
SE-75	121,12	1,166	1,170
	136	1,169	1,170
	264,66	1,143	1,140
	279,54	1,092	1,090
	400,66	0,624	0,633
Y-88	898.02	1,085	1,090
	1836,01	1,096	1,090
RH-106	511.70	1,070	1,070
AG-110M	657.76	1,269	1,270
	706,68	1,368	1,370
	884,68	1,268	1,270
	937,49	1,258	1,260
	1384,3	1,200	1,200
I-131	364,49	1,000	1,000
BA-133	81	1,164	1,170
	302,84	1,072	1,070
	356,01	1,051	1,050
CS-134	604,72	1,144	1,140
	795,86	1,141	1,140
EU-152	121.78	1,121	1,120
	344,27	1,083	1,080
	1085,78	0,957	0,959
	1407,95	1,048	1,050
TL-208	583,19	1,117	1,120
BI-212	727.33	1,032	1,030
	1620,5	0,991	0,991
BI-214	609.31	1,099	1,100
	1120,29	1,114	1,110
	1764,49	0,998	0,998
AC-228	338.32	1,002	1,000
	911,2	1,015	1,010
	968,97	1,013	1,010
PA-233	312,17	1,003	1,000

Detector 3: Pellets (1g/cm^3)

Nuclide	Energy (keV)	5 mm thickness	10 mm thickness	20 mm thickness
CO-60	1173.23	1,218	1,190	1,160
	1332,49	1,229	1,200	1,170
SE-75	121,12	1,381		
	136	1,395		
	264,66	1,362		
	279,54	1,225		
	400,66	0,366		
Y-88	898.02	1,189	1,170	1,140
	1836,01	1,235	1,210	1,170
RH-106	511.70	1,158	1,140	1,120
AG-110M	657.76	1,663	1,580	1,470
	706,68	1,958	1,820	1,670
	884,68	1,681	1,590	1,480
	937,49	1,660	1,570	1,470
	1384,3	1,517	1,450	1,370
I-131	364,49	1,000	1,000	1,000
BA-133	81	1,360	1,310	1,260
	302,84	1,176	1,150	1,120
	356,01	1,124	1,110	1,090
CS-134	604,72	1,339	1,300	1,250
	795,86	1,345	1,300	1,250
EU-152	121.78	1,253	1,220	1,190
	344,27	1,184	1,160	1,140
	1085,78	0,899	0,910	0,925
	1407,95	1,126	1,110	1,090
TL-208	583,19	1,259	1,230	1,190
BI-212	727.33	1,072	1,060	1,050
	1620,5	0,980	0,982	0,985
BI-214	609.31	1,226	1,200	1,170
	1120,29	1,283	1,250	1,200
	1764,49	0,995	0,996	0,997
AC-228	338.32	1,002	1,000	1,000
	911,2	1,033	1,030	1,020
	968,97	1,028	1,030	1,020
PA-233	312,17	1,008	1,010	1,010

Detector 3: Pellets (1.5g/cm^3)

Nuclide	Energy (keV)	5 mm thickness	10 mm thickness	20 mm thickness
CO-60	1173.23	1,216	1,190	1,160
	1332,49	1,227	1,200	1,160
SE-75	121,12	1,372		
	136	1,385		
	264,66	1,351		
	279,54	1,218		
	400,66	0,373		
Y-88	898.02	1,188	1,170	1,140
	1836,01	1,232	1,200	1,170
RH-106	511.70	1,155	1,140	1,110
AG-110M	657.76	1,654	1,560	1,460
	706,68	1,942	1,800	1,650
	884,68	1,671	1,570	1,470
	937,49	1,650	1,560	1,450
	1384,3	1,509	1,440	1,360
I-131	364,49	1,000	1,000	1,000
BA-133	81	1,352	1,300	1,250
	302,84	1,170	1,140	1,120
	356,01	1,121	1,100	1,080
CS-134	604,72	1,334	1,290	1,240
	795,86	1,339	1,290	1,240
EU-152	121.78	1,249	1,220	1,180
	344,27	1,181	1,160	1,130
	1085,78	0,902	0,914	0,930
	1407,95	1,123	1,100	1,080
TL-208	583,19	1,257	1,230	1,190
BI-212	727.33	1,071	1,060	1,050
	1620,5	0,980	0,982	0,985
BI-214	609.31	1,223	1,200	1,160
	1120,29	1,278	1,240	1,200
	1764,49	0,996	0,996	0,997
AC-228	338.32	1,002	1,000	1,000
	911,2	1,033	1,030	1,020
	968,97	1,028	1,020	1,020
PA-233	312,17	1,007	1,010	1,010

Detector 4: Marinelli beaker

Nuclide	Energy (keV)	0.5 L (1g/cm^3)	0.5 L (1.5g/cm^3)	1 L (1g/cm^3)	1 L (1.5g/cm^3)
CO-60	1173.23	1,094	1,092	1,078	1,076
	1332,49	1,094	1,092	1,078	1,076
SE-75	121,12	1,131	1,127	1,123	1,104
	136	1,133	1,129	1,110	1,105
	264,66	1,121	1,115	1,097	1,092
	279,54	1,077	1,074	1,063	1,059
	400,66	0,645	0,658	0,695	0,712
Y-88	898.02	1,090	1,089	1,075	1,074
	1836,01	1,090	1,088	1,074	1,072
RH-106	511.70	1,062	1,059	1,051	1,049
AG-110M	657.76	1,236	1,231	1,195	1,190
	706,68	1,311	1,303	1,254	1,246
	884,68	1,235	1,229	1,193	1,187
	937,49	1,224	1,217	1,183	1,177
	1384,3	1,175	1,170	1,144	1,139
I-131	364,49	1,000	1,000	1,000	1,000
BA-133	81	1,122	1,118	1,068	1,098
	302,84	1,030	1,028	1,024	1,023
	356,01	1,028	1,026	1,023	1,021
CS-134	604,72	1,125	1,122	1,104	1,101
	795,86	1,122	1,118	1,100	1,097
EU-152	121.78	1,105	1,103	1,108	1,087
	344,27	1,073	1,071	1,061	1,059
	1085,78	0,967	0,969	0,974	0,975
	1407,95	1,044	1,042	1,035	1,032
TL-208	583,19	1,125	1,123	1,104	1,102
BI-212	727.33	1,030	1,030	1,025	1,024
	1620,5	0,991	0,991	0,992	0,993
BI-214	609.31	1,093	1,091	1,077	1,076
	1120,29	1,100	1,097	1,083	1,079
	1764,49	0,998	0,998	0,998	0,998
AC-228	338.32	1,002	1,002	1,002	1,002
	911,2	1,012	1,012	1,010	1,010
	968,97	1,012	1,012	1,010	1,010
PA-233	312,17	1,002	1,002	1,002	1,002

Detector 4: Plastic Bottle (0,5L)

Nuclide	Energy (keV)	1g/cm^3	1.5g/cm^3
CO-60	1173.23	1,094	1,085
	1332,49	1,094	1,085
SE-75	121,12	1,131	1,138
	136	1,133	1,140
	264,66	1,121	1,128
	279,54	1,077	1,082
	400,66	0,645	0,680
Y-88	898.02	1,090	1,084
	1836,01	1,090	1,079
RH-106	511.70	1,062	1,058
AG-110M	657.76	1,236	1,228
	706,68	1,311	1,299
	884,68	1,235	1,220
	937,49	1,224	1,207
	1384,3	1,175	1,157
I-131	364,49	1,000	1,000
BA-133	81	1,122	1,127
	302,84	1,030	1,032
	356,01	1,028	1,030
CS-134	604,72	1,125	1,119
	795,86	1,122	1,113
EU-152	121.78	1,105	1,110
	344,27	1,073	1,072
	1085,78	0,967	0,970
	1407,95	1,044	1,040
TL-208	583,19	1,125	1,124
BI-212	727.33	1,030	1,028
	1620,5	0,991	0,992
BI-214	609.31	1,093	1,089
	1120,29	1,100	1,090
	1764,49	0,998	0,998
AC-228	338.32	1,002	1,002
	911,2	1,012	1,011
	968,97	1,012	1,011
PA-233	312,17	1,002	1,002

Detector 4: Pellets (1g/cm^3)

Nuclide	Energy (keV)	5 mm thickness	10 mm thickness	20 mm thickness
CO-60	1173.23	1,194	1,144	1,140
	1332,49	1,198	1,146	1,142
SE-75	121,12	1,307	1,218	1,210
	136	1,315	1,223	1,215
	264,66	1,308	1,216	1,204
	279,54	1,189	1,135	1,128
	400,66	0,446	0,530	0,548
Y-88	898.02	1,187	1,139	1,137
	1836,01	1,191	1,140	1,136
RH-106	511.70	1,127	1,094	1,092
AG-110M	657.76	1,535	1,384	1,375
	706,68	1,740	1,519	1,504
	884,68	1,538	1,383	1,372
	937,49	1,513	1,364	1,353
	1384,3	1,395	1,282	1,274
I-131	364,49	1,000	1,000	1,000
BA-133	81	1,274	1,195	1,190
	302,84	1,068	1,051	1,048
	356,01	1,065	1,048	1,045
CS-134	604,72	1,270	1,197	1,192
	795,86	1,267	1,193	1,188
EU-152	121.78	1,219	1,162	1,159
	344,27	1,150	1,112	1,109
	1085,78	0,927	0,946	0,949
	1407,95	1,105	1,075	1,071
TL-208	583,19	1,265	1,197	1,194
BI-212	727.33	1,060	1,045	1,044
	1620,5	0,981	0,986	0,987
BI-214	609.31	1,194	1,143	1,139
	1120,29	1,220	1,158	1,153
	1764,49	0,996	0,997	0,997
AC-228	338.32	1,002	1,002	1,002
	911,2	1,025	1,019	1,018
	968,97	1,025	1,018	1,018
PA-233	312,17	1,004	1,003	1,003

Detector 4: Pellets (1.5 g/cm^3)

Nuclide	Energy (keV)	5 mm thickness	10 mm thickness	20 mm thickness
CO-60	1173.23	1,207	1.169	1.140
	1332,49	1,197	1.170	1.142
SE-75	121,12	1.283	1.257	1.210
	136	1.316	1.264	1.215
	264,66	1.296	1.254	1.204
	279,54	1.204	1.157	1.128
	400,66	0.411	0.491	0.548
Y-88	898.02	1,187	1.163	1.137
	1836,01	1.197	1.165	1.136
RH-106	511.70	1,132	1.110	1.092
AG-110M	657.76	1,569	1.456	1.375
	706,68	1.79	1.621	1.504
	884,68	1,568	1.455	1.372
	937,49	1,543	1.434	1.353
	1384,3	1,431	1.335	1.274
I-131	364,49	1,000	1.000	1.000
BA-133	81	1,257	1.231	1.190
	302,84	1,071	1.058	1.048
	356,01	1,069	1.055	1.045
CS-134	604,72	1,251	1.232	1.192
	795,86	1,258	1.228	1.188
EU-152	121.78	1,224	1.189	1.159
	344,27	1,156	1.131	1.109
	1085,78	0,941	0.938	0.930
	1407,95	1,094	1.088	1.071
TL-208	583,19	1,255	1.231	1.194
BI-212	727.33	1,063	1.053	1.044
	1620,5	0,998	0.984	0.987
BI-214	609.31	1,203	1.168	1.139
	1120,29	1,228	1.188	1.153
	1764,49	0,997	0.997	0.997
AC-228	338.32	1,005	1.003	1.002
	911,2	1,025	1.021	1.018
	968,97	1,025	1.022	1.018
PA-233	312,17	1,003	1.004	1.003

Detector 5: Marinelli beaker

Nuclide	Energy (keV)	0.5 L (1g/cm^3)	0.5 L (1.5g/cm^3)	1 L (1g/cm^3)	1 L (1.5g/cm^3)
CO-60	1173.23	1,111	1,109	51230	52230
	1332,49	1,113	1,110	1,092	1,090
SE-75	121,12			1,093	1,091
	136				
	264,66				
	279,54				
	400,66				
Y-88	898.02	1,103	1,101		
	1836,01			1,086	1,084
RH-106	511.70	1,072	1,071		
AG-110M	657.76	1,288	1,281	1,060	1,059
	706,68	1,380	1,370	1,237	1,230
	884,68	1,285	1,277	1,310	1,301
	937,49	1,272	1,264	1,233	1,225
	1384,3	1,219	1,213	1,222	1,215
I-131	364,49	1,000	1,000	1.18	1,174
BA-133	81	1,134	1,130	1,000	1,000
	302,84	1,025	1,024	1,110	1,108
	356,01	1,024	1,023	1,021	1,019
CS-134	604,72	1,151	1,146	1,019	1,018
	795,86	1,145	1,141	1,124	1,121
EU-152	121.78	1,123	1,121	1,119	1,115
	344,27	1,086	1,084	1,103	1,101
	1085,78	0,968	0,971	1,072	1,070
	1407,95	1,036	1,034	0,975	0,977
TL-208	583,19	1,137	1,135	1,029	1,026
BI-212	727.33	1,036	1,035	1,114	1,112
	1620,5	0,991	0,991	1,030	1,029
BI-214	609.31	1,111	1,108	0,993	0,992
	1120,29	1,120	1,116	1,092	1,090
	1764,49	0,998	0,998	1,098	1,095
AC-228	338.32	1,004	1,004	0,999	0,999
	911,2	1,014	1.01	1,003	1,004
	968,97	1,014	1,014	1,012	1,011
PA-233	312,17	1,002	1,002	1,012	1,011

Detector 5: Plastic Bottle (0,5L)

Nuclide	Energy (keV)	1g/cm^3	1.5g/cm^3
CO-60	1173.23	1,101	1,101
	1332,49	1,102	1,102
SE-75	121,12		
	136		
	264,66		
	279,54		
	400,66		
Y-88	898.02	1,095	1,097
	1836,01		
RH-106	511.70	1,069	1,070
AG-110M	657.76	1,277	1,279
	706,68	1,370	1,370
	884,68	1,270	1,269
	937,49	1,255	1,254
	1384,3	1,200	1,198
I-131	364,49	1,000	1,000
BA-133	81	1,137	1,140
	302,84	1,027	1,027
	356,01	1,026	1,025
CS-134	604,72	1,143	1,144
	795,86	1,136	1,135
EU-152	121.78	1,125	1,130
	344,27	1,084	1,085
	1085,78	0,970	0,971
	1407,95	1,035	1,033
TL-208	583,19	1,133	1,136
BI-212	727.33	1,033	1,033
	1620,5	0,992	0,992
BI-214	609.31	1,105	1,107
	1120,29	1,109	0,111
	1764,49	0,999	0,999
AC-228	338.32	1,003	1,003
	911,2	1,013	1,013
	968,97	1,013	1,013
PA-233	312,17	1,002	1,002

Detector 5: Pellets (1g/cm^3)

Nuclide	Energy (keV)	5 mm thickness	10 mm thickness	20 mm thickness
CO-60	1173.23	1.23	1,232	1,232
	1332,49	1,241	1,238	1,238
SE-75	121,12			
	136			
	264,66			
	279,54			
	400,66			
Y-88	898.02	0,122	1,214	1,214
	1836,01			
RH-106	511.70	1,152	1,150	1,150
AG-110M	657.76	1.68	1.67	1.67
	706,68	1.95	1.93	1.93
	884,68	1,677	1,665	1,665
	937,49	1,647	1,636	1,636
	1384,3	1,513	1,505	1,505
I-131	364,49	1,000	1,000	1,000
BA-133	81	1,306	1,300	1,300
	302,84	1,057	1,055	1,055
	356,01	1,054	1,052	1,052
CS-134	604,72	1.33	1.33	1.33
	795,86	1.33	1,321	1,321
EU-152	121.78	1,259	1,256	1,256
	344,27	1,180	1,178	1,178
	1085,78	0,931	0,933	0,933
	1407,95	1,085	1,083	1,083
TL-208	583,19	1,293	1,290	1,290
BI-212	727.33	1,071	1,070	1,070
	1620,5	0,982	0,982	0,982
BI-214	609.31	0,124	1,232	1,232
	1120,29	1,268	1,264	1,264
	1764,49	0,997	0,997	0,997
AC-228	338.32	1,005	1,005	1,005
	911,2	1,029	1,028	1,028
	968,97	1,028	1,028	1,028
PA-233	312,17	1,004	1,004	1,004

Detector 5: Pellets (1.5g/cm^3)

Nuclide	Energy (keV)	5 mm thickness	10 mm thickness	20 mm thickness
CO-60	1173.23	1,232	1,232	1,202
	1332,49	1,238	1,238	1,207
SE-75	121,12			
	136			
	264,66			
	279,54			
	400,66			
Y-88	898.02	1,214	1,214	1,187
	1836,01			
RH-106	511.70	1,150	1,150	1,132
AG-110M	657.76	1.67	1.67	1,569
	706,68	1.93	1.93	1.79
	884,68	1,665	1,665	1,568
	937,49	1,636	1,636	1,543
	1384,3	1,505	1,505	1,431
I-131	364,49	1,000	1,000	1,000
BA-133	81	1,300	1,300	1,257
	302,84	1,055	1,055	1,048
	356,01	1,052	1,052	1,046
CS-134	604,72	1.33	1.33	1,284
	795,86	1,321	1,321	1,278
EU-152	121.78	1,256	1,256	1,224
	344,27	1,178	1,178	1,156
	1085,78	0,933	0,933	0,941
	1407,95	1,083	1,083	1,071
TL-208	583,19	1,290	1,290	1,255
BI-212	727.33	1,070	1,070	1,063
	1620,5	0,982	0,982	0,984
BI-214	609.31	1,232	1,232	1,203
	1120,29	1,264	1,264	1,228
	1764,49	0,997	0,997	0,997
AC-228	338.32	1,005	1,005	1,005
	911,2	1,028	1,028	1,025
	968,97	1,028	1,028	1,025
PA-233	312,17	1,004	1,004	1,003

Detector 6: Marinelli beaker

Nuclide	Energy (keV)	0.5 L (1g/cm^3)	0.5 L (1.5g/cm^3)	1 L (1g/cm^3)	1 L (1.5g/cm^3)
CO-60	1173.23	1,096	1,093	1,080	1,077
	1332,49	1,097	1,095	1,081	1,078
SE-75	121,12	1,000	1,000	1,000	1,000
	136	1,127	1,122	1,104	1,101
	264,66	1,128	1,123	1,105	1,101
	279,54	1,099	1,095	1,081	1,076
	400,66	1,062	1,060	1,051	1,048
Y-88	898.02	1,000	1,000	1,000	1,000
	1836,01	1,089	1,087	1,074	1,073
RH-106	511.70	1,094	1,092	1,078	1,075
AG-110M	657.76	1,000	1,000	1,000	1,000
	706,68	1,247	1,240	1,203	1,198
	884,68	1,325	1,316	1,267	1,258
	937,49	1,245	1,238	1,201	1,195
	1384,3	1,234	1,228	1,192	1,185
I-131	364,49	1,185	1,179	1,152	1,147
BA-133	81	1,121	1,117	1,100	1,097
	302,84	1,121	1,117	1,100	1,097
	356,01	1,024	1,023	1,020	1,018
CS-134	604,72	1,023	1,022	1,018	1,017
	795,86	1,131	1,127	1,108	1,105
EU-152	121.78	1,107	1,105	1,090	1,089
	344,27	1,075	1,074	1,063	1,061
	1085,78	0,967	0,969	0,974	0,975
	1407,95	1,035	1,033	1,028	1,026
TL-208	583,19	1,000	1,000	1,000	1,000
BI-212	727.33	1,000	1,000	1,000	1,000
	1620,5	1,000	1,000	1,000	1,000
BI-214	609.31	1,000	1,000	1,000	1,000
	1120,29	1,000	1,000	1,000	1,000
	1764,49	1,000	1,000	1,000	1,000
AC-228	338.32	1,002	1,002	1,002	1,002
	911,2	1,013	1,012	1,010	1,010
	968,97	1,013	1,012	1,010	1,010
PA-233	312,17	1,002	1,002	1,001	1,001

Detector 6: Plastic Bottle (0,5L)

Nuclide	Energy (keV)	1g/cm^3	1.5g/cm^3
CO-60	1173.23	1,087	1,087
	1332,49	1,088	1,088
SE-75	121,12	1,000	1,000
	136	1,132	1,134
	264,66	1,133	1,134
	279,54	1,107	1,105
	400,66	1,067	1,066
Y-88	898.02	1,000	1,000
	1836,01	1,082	1,083
RH-106	511.70	1,084	1,082
AG-110M	657.76	1,000	1,000
	706,68	1,236	1,237
	884,68	1,313	1,314
	937,49	1,230	1,229
	1384,3	1,218	1,217
I-131	364,49	1,168	1,166
BA-133	81	1,123	1,126
	302,84	1,123	1,126
	356,01	1,027	1,027
CS-134	604,72	1,025	1,024
	795,86	1,124	1,124
EU-152	121.78	1,109	1,112
	344,27	1,073	1,074
	1085,78	0,968	0,970
	1407,95	1,034	1,031
TL-208	583,19	1,000	1,000
BI-214	609.31	1,000	1,000
	1120,29	1,000	1,000
	1764,49	1,000	1,000
AC-228	338.32	1,002	1,002
	911,2	1,011	1,011
	968,97	1,011	1,011
PA-233	312,17	1,002	1,002

Detector 6: Pellets (1g/cm^3)

Nuclide	Energy (keV)	5 mm thickness	10 mm thickness	20 mm thickness
CO-60	1173.23	1,198	1,197	1,175
	1332,49	1,204	1,202	1,180
SE-75	121,12	1,000	1,000	1,000
	136	1,294	1,288	1,255
	264,66	1,299	1,292	1,259
	279,54	1,247	1,240	1,213
	400,66	1,149	1,145	1,130
Y-88	898.02	1,000	1,000	1,000
	1836,01	1,183	1,182	1,162
RH-106	511.70	1,201	1,198	1,175
AG-110M	657.76	1,000	1,000	1,000
	706,68	1,562	1,554	1,487
	884,68	1,781	1,768	1,671
	937,49	1,565	1,556	1,488
	1384,3	1,541	1,532	1,468
I-131	364,49	1,420	1,414	1,364
BA-133	81	1,270	1,265	1,234
	302,84	1,270	1,265	1,234
	356,01	1,056	1,054	1,050
CS-134	604,72	1,052	1,051	1,046
	795,86	1,283	1,279	1,248
EU-152	121.78	1,222	1,219	1,196
	344,27	1,156	1,154	1,138
	1085,78	0,928	0,930	0,936
	1407,95	1,083	1,080	1,072
TL-208	583,19	1,000	1,000	1,000
BI-212	727.33	1,000	1,000	1,000
	1620,5	1,000	1,000	1,000
BI-214	609.31	1,000	1,000	1,000
	1120,29	1,000	1,000	1,000
	1764,49	1,000	1,000	1,000
AC-228	338.32	1,003	1,003	1,003
	911,2	1,026	1,025	1,023
	968,97	1,025	1,025	1,022
PA-233	312,17	1,004	1,004	1,003

Detector 6: Pellets (1.5g/cm^3)

Nuclide	Energy (keV)	5 mm thickness	10 mm thickness	20 mm thickness
CO-60	1173.23	1,197	1,175	1,173
	1332,49	1,202	1,180	1,176
SE-75	121,12	1,000	1,000	1,000
	136	1,288	1,255	1,247
	264,66	1,292	1,259	1,251
	279,54	1,240	1,213	1,204
	400,66	1,145	1,130	1,125
Y-88	898.02	1,000	1,000	1,000
	1836,01	1,182	1,162	1,160
RH-106	511.70	1,198	1,175	1,172
AG-110M	657.76	1,000	1,000	1,000
	706,68	1,554	1,487	1,477
	884,68	1,768	1,671	1,655
	937,49	1,556	1,488	1,478
	1384,3	1,532	1,468	1,457
I-131	364,49	1,414	1,364	1,356
BA-133	81	1,265	1,234	1,228
	302,84	1,265	1,234	1,228
	356,01	1,054	1,050	1,048
CS-134	604,72	1,051	1,046	1,044
	795,86	1,279	1,248	1,244
EU-152	121.78	1,219	1,196	1,193
	344,27	1,154	1,138	1,135
	1085,78	0,930	0,936	0,938
	1407,95	1,080	1,072	1,069
TL-208	583,19	1,000	1,000	1,000
BI-212	727.33	1,000	1,000	1,000
	1620,5	1,000	1,000	1,000
BI-214	609.31	1,000	1,000	1,000
	1120,29	1,000	1,000	1,000
	1764,49	1,000	1,000	1,000
AC-228	338.32	1,003	1,003	1,003
	911,2	1,025	1,023	1,022
	968,97	1,025	1,022	1,022
PA-233	312,17	1,004	1,003	1,003

References

[1] Radiation Detection and Measurements, By Glenn F. Knoll, John Wiley (1979 and 1989).

[2] Gamma and X-ray Spectrometry with Semiconductor Detector, By Debertin and R. G. Helmer , North Holland(1988)

[3] http://www.canberra.com/literature/931.asp

[4] R. D. Evans, The Atomic Nucleus, (McGraw-Hill Book Company, 1955).

[5] ORTEC How Counting Statistics Controls Detection Limits and Peak Precision http://www.ortec-online.com/ application-notes/an59.pdf

[6] http--www4.nau.edu-microanalysis-Microprobe-img

[7] X-ray and Gamma-ray Standards for the Detector Calibration, IAEA TECDOC-619 (1991

[8] Assessments of the NPL intercomparison
Jerome, S. (1990). Environmental radioactivity intercomparison exercise, Report RSA (EXT) 5, National Physical Laboratory, Teddington.
Jerome, S. (1991). Environmental radioactivity intercomparison exercise, Report RSA (EXT) 20, National Physical Laboratory, Teddington.
Jerome, S. , Woods, M. J., Lucas, S. E. M. and Hooley (1993). Environmental radioactivity intercomparison exercise, Report RSA 37EXT) 5, National Physical Laboratory, Teddington

[9] Table of Radioactive Isotopes, by E. Browne and R.B Firestone, John Wiley (1986).

[10] The performance of the well-established programs available to perform summing Corrections (CASUCO, KORSUM, and COSUCO) are discussed by:
Jedlovsky, R. (1981). Report OMH 8301 (ICRM-S-10), National office of Measure, Budapest, Hungary.

[11] D. S. ANDREEV, K. I. EROKHINA, V. S. ZVONOV, I. Kh. LEMBERG, Instr. Expt. Techn., !5 (1972)1358.

[12]. D. S. ANDREEV, K. I. EROKHINA, V. S. ZVONOV, 1. Kh. LEMBERG, Izv. Akad. Nauk SSSR, Ser.Fiz., 37 (1973) No. 8, 1609.

[13] V. P. Kolotov, *+ M. J. Koskelo** Testing of different true coincidence correction approaches for gamma-ray spectrometry of voluminous sources

[14] Canberra Genie 2000 Basic Spectroscopy Software

[15] Canberra Genie 2000 Analysis Software

[16] LabSOCS Calibration Software

[17] Measurements and Detection of radiation, Nicholas Tsoulfandis-Washington Hemisphere Publ. Corp. 1983

[18] www.drct.com

[19] http://www.canberra.com/products/476.asp

[20] Radioactivity Measurements Principles and Practice, by W. B. Mann, A Rytz, A Spernol , Pergamon Press (1991)

[21] American National Standard Institute/Institute of Electric and Electronic Engineers. (ANSI/IEEE) 325.Standard Test Procedure for Germanium Gamma-Ray Detector, 1996, New York

[22] http--www4.nau.edu-microanalysis-Microprobe-img

[23] M. J. Koskelo,*+ R. Venkataraman,* V. P. Kolotov**, Coincidence Correction Summing using alternative detector characterization data

[24] V. P. KOLOTOV, V. V. ATRASHKEVICH, N. N. DOGADKIN, MAPPING OF TRUE COINCIDENCE EFFECT VALUE FOR VOLUMINOUS SOURCES MEASURED WITH HPGE

[25] F. DE Corte , The correction for γ-γ, γ-LX true coincidence in Ko standardized VAA with counting in a LEPD

[26] Marc Décamba~, Jean-Jacques Grostely and Jean-Pascal Laedermann, coincidence summing correction for extended sources in gamma spectroscopy using Monte- Carlo simulation

[26] Mauro S. Dias*, Mauro N. Takeda, Marina F. Koskinas, Cascade summing corrections for HPGe spectrometers by the Monte Carlo method

[27] Peter N. Johnston, Mikael Hult Joe¨ l Gasparro, Cascade summing effects in close geometry gamma-ray spectrometry

[28] I. Ramos-Lerate", M. Barrera, R.A. Ligero, M. Casas-Ruiz, A new summing-correction method for gamma-efficiency calibration with multi-gamma-ray radionuclides

[29] F. J. SCHIMA~ and D. D. HOPPES, TABLES FOR CASCADE-SU~41NG CORRECTIONS IN GAMMA-RAY SPECTRO~TRZ

[30] Zhonglu Wang, Bernd Kahn, and John D. Valentine, Member, IEEE, Efficiency Calculation and Coincidence Summing Correction for Germanium Detectors by Monte Carlo Simulation